

**Using Remote Sensing for Quantity
Analysis of Chip Pile Inventory in Mill Yards**

by

Benjamin P. Ong

A Graduate Thesis Submitted in Partial Fulfillment of the
Requirements for the Master's Degree of Science in Forestry

Faculty of Natural Resources Management

Lakehead University

December 2016

LIBRARY RIGHTS STATEMENT

In presenting this thesis in partial fulfillment of the requirements for the M.Sc.F. degree at Lakehead University in Thunder Bay, I agree that the University will make it freely available for inspection.

This thesis is made available by my authority solely for the purpose of private study and research and may not be copied or reproduced in whole or in part (except as permitted by the Copyright Laws) without my written authority.

Signature _____

Date _____

A CAUTION TO THE READER

This Master of Science of Forestry thesis has been through a semi-formal process of review and comment by at least two faculty members.

It is made available for loan by the faculty for the purpose of advancing the practice of professional and scientific forestry.

The reader should realize that the opinions expressed in this document are the opinions and conclusions of the student and do not necessarily reflect the opinions of the supervisor, the Faculty, or the University.

ACKNOWLEDGEMENTS

I would like to thank my thesis advisor Dr. Ulf Runesson of the Faculty of Natural Resources Management and my committee advisors Dr. Mathew Leitch, and Dr. Chander Shahi for their insight and support throughout my Master's research. Their guidance allowed me to develop and finish my research by steering me in the right direction whenever I needed it. I would also like to acknowledge the assistants of Mr. Alex Bilyk and Ms. Andrea Collins for their occasional inputs, which helped with the progress of my research. While they are not officially on my committee, their occasional advice was greatly appreciated.

I would also like to acknowledge the contributions of NSERC for their grants and support that made this whole thesis possible, as well as their part in encouragement of industry-partners to work with me making the concepts in this thesis applicable to real world situations. These included CCS (Central Computer Services Inc.) as my main industry-partner in this project, AV Terrace Bay, Resolute Forest Products for their donations, and access to their mills for real world testing, and finally Sumac Geomatics Inc. for their aerial imagery of some of the chip piles.

Thanks to all of you for your advice, assistance, support, and guidance for without everyone, this research project would not have happened.

ABSTRACT

Ong, Benjamin P. 2016. Using Remote Sensing for Quantity Analysis of Chip Pile Inventory in Mill Yards. 75pp.

An integral part of proper wood chip inventory management is the ability to accurately monitor wood chip quantities. This thesis examines the use of a new method of capturing the volume of mill yard wood chip piles through the utilization of aerial drones. The drones are used to capture images and the images are converted into digital 3D models, which are then capable of measuring pile volume. This process allows for conversion of the volume into an accurate mass estimate by compensating for compression factors within the chip pile. These factors can change the volume by a maximum of 9.46%, but on average during simulations and real world applications, most piles exhibit a change in volume in the range of 1% to 6% difference. By performing the estimation procedure multiple times and averaging the results this method is able to generate a result that is more precise, timely and less labour intensive than the previous methods of using a ground survey to determine volume and applying a linear volume to mass conversion for the quantity of wood chips. The results suggest that this averaging technique can improve the standard deviation spread from over 5% variation in the measurement to less than 2%. This new method combines multiple techniques to improve both overall accuracy and precision. Each stage of the new method was examined to

determine the accumulated degree of error. This included looking at operator error of about 2.4%, considering the precision of 3D volume capture, which adds on average of 5% to 10% error, understanding the variation in bulk density due to pile shape, and size, which adds 1% to 6% error, using different 3D software modeling for measuring pile volume, which adds about 4% error. Combined together in extreme cases, these errors can skew the results by over 20%. The results of this examination provides research-based recommendations as to how to collect the images, generate the models, and process the data for mass estimation and improve error reduction at all stages.

Keywords: 3D model capture, bulk density, compression forces, error reduction, mass estimation, mill yard inventory, UAV imagery, volume loss, wood-chip pile.

CONTENTS

LIBRARY RIGHTS STATEMENT	ii
A CAUTION TO THE READER	iii
ACKNOWLEDGEMENTS	iv
ABSTRACT.....	v
CONTENTS	vii
TABLES.....	ix
FIGURES.....	xi
EQUATIONS.....	xiii
INTRODUCTION	1
Objective of the study	2
A synopsis of the stages in this study	2
LITERATURE REVIEW	8
Volume Capture Using Stereo Imagery Analysis Software	8
Global Positional System (GPS) Location Capture Accuracy	9
Compression Force Distribution in Piles of Particles	11
Loss of Wood Fibre During Storage in Mill Yards	13
Economic Impacts of Inventory Management in Mill Yards.....	14
METHODOLOGY	15
Phase I (Development of the Compression Curve).....	15
Phase II (Proof of Concept on a Small Scale).....	19
Phase III (Medium Scale Analysis)	25
Phase IV (Error Analysis and Large Scale Predictions).....	29
RESULTS	32
Compression, Decompression, and Time Compression Curves.....	32
Small Scale Chip Pile Volumetric and Mass Estimations.....	36
Medium Scale Analysis.....	39
Prediction of Compression Force Distribution in a Chip Pile with Cross-Section Modeling.....	42
Error Identification and Reduction Analysis	45
Large Scale Skew	45

.....	46
Monte Carlo Simulation of Mass Estimates Improved by Averaging Method.....	47
Calculating Error of Operator.....	49
Calculating Error due to Software.....	50
Compensation Error due to Decompression.....	51
DISCUSSION.....	52
Developing the Control Metrics and Variables.....	52
Volume loss due to Shape, Height and Bulk Density.....	55
Decompression Requires an Additional Correction Factor.....	57
Stabilization Period Required for Accurate Mass Estimation.....	59
Differences between Basic Linear Conversion method (BLC) and Compression Compensated Conversion method (CCC).....	60
Application of Method in a Mill Environment.....	61
Error Distribution in Volume Measurements and Mass Estimations.....	63
Accuracy Errors due to Image Scale Calibration of the 3D Model....	68
Accuracy Errors due to Software Algorithms for Generating 3D Models.....	70
CONCLUSION.....	71
LITERATURE CITED.....	74

TABLES

Table 1: Descriptive statistics for a small conical pile showing the difference between BLC and CCC conversion methods.....	38
Table 2: Descriptive statistics for a small-flattened pile showing the difference between BLC and CCC conversion methods.....	38
Table 3: Chart examining the F statistics and significance level of mass estimation between BLC and CCC conversion methods, for conical chip and flattened chip piles.	39
Table 4: Daily mass estimations of three chip piles at a local mill comparing the differences between CCC method and the mills method.....	41
Table 5: Comparison of the mass estimates on Table 4 sorted and averaged based on the conical and flattened pile shapes.	42
Table 6: Chart showing the difference between CCC and mill estimates for both conical and flattened pile shapes when increasing the size of the pile by factors of 27 and 1000.....	45
Table 7: Chart showing the total average, standard deviation, and percentage of the 10,000 Monte Carlo simulated estimates which fall within 3% and 5% of the actual mass when the predicted masses have been generated using the average of multiple estimates of conical piles.....	48
Table 8: Chart showing the total average, standard deviation, and percentage of the 10,000 Monte Carlo simulated estimates which fall within 3% and 5% of the actual mass when the predicted masses have been generated using the average of multiple estimates of flattened piles.	49
Table 9: Comparison of the variation of answers when the same photo set is reprocessed using the same procedure to examine deviation due to operator error, both in the Z axis and in the X,Y,Z axis.....	50

Table 10: Chart showing descriptive stats of the difference between estimates generated using different software processing identical image sets.	50
--	----

FIGURES

Figure 1: Three 44-imperial gallon barrels used for compression and decompression testing.....	18
Figure 2: One cubic meter container used for measuring the wood chips on a small scale pile.	20
Figure 3: Small-scale wood chip pile shaped into a conical shape.	21
Figure 4: Small-scale pile reshaped into a flattened pile.....	22
Figure 5: 3D model of the chip pile showing the location of all the camera locations.	23
Figure 6: Transition from photo image to 3D model on the computer for both conical and flattened piles.	24
Figure 7: Aerial view of the chip pile at the mill in Longlac taken using a Phantom II - DJI drone.	26
Figure 8: Overhead Drone Photo of the chip pile in Thunder Bay.....	28
Figure 9: Graph showing the percentage of volume loss due to static compression applied over time.	33
Figure 10: Graph showing the range of wood chip decompression over time.....	34
Figure 11: Chart showing the volume loss due to pressure applied on to the wood chips.....	35
Figure 12: 3D model of the chip piles on Monday June 15.	40
Figure 13: 3D model of the chip piles on Tuesday June 16.	40
Figure 14: 3D model of the chip pile on Thursday June 18.....	40
Figure 15: 3D model of the chip piles on Friday June 19.	41
Figure 16: Showing the different varying densities of wood chips throughout a chip pile as shape varies from a square pile, a flattened pile, and a tall pile in a silo.	43
Figure 17: Showing the different varying densities of wood chips as the pile changes in height.	44

Figure 18: Showing the different varying densities of wood chips as the bulk density changes.	44
Figure 19: Graphic models of compression distribution in the predicted conical piles of Table 6.	46
Figure 20: Graphic models of compression distribution in the predicted flattened piles of Table 6.	47
Figure 21: Showing the different varying densities of wood chips as one pile goes through decompression while the other pile is formed normally.	51
Figure 22: Sample of GPS error when compared to ground control points exaggerated by 1000 times	69

EQUATIONS

Equation 1 - Volume loss due to compression load	36
Equation 2 - First derivative of equation 1	36
Equation 3 - Volume to mass conversion using BLC Method	37
Equation 4 - Volume to mass conversion using CCC Method.....	37

INTRODUCTION

Inventory management is crucial to the smooth and efficient operation of the manufacturing process in any industry. For the pulp and paper industry, it has become a recognized fact that the inaccuracies in determining the quantity of wood chips in their yard piles can cause significant financial challenges. These inaccuracies are a result of differences between the mass of the chips delivered by trucks to the mill, surveyed quantities of the chip pile inventory in the mill yards, and estimated mass of chips consumed during the operations of the boilers. In total, these discrepancies can add up to millions of dollars of unaccountable wood chips each year at each mill. The current sources of mass estimation are visual scale estimation, truckload logistics, and ground surveys of the wood chip piles. The discrepancies that are found between the three methods are the reason that is driving this study of wood chip mass estimation using remote sensing imagery. The general desire voiced by many mills was to have a simple and accurate method of chip inventory estimation that can be implemented regularly. In addition, the new method developed would also be more cost effective to allow for an increase in the frequency of these inventories, as well as increased safety of the survey crews performing the surveys. This was to be accomplished without interfering with daily mill operations while still improving the accuracy and precision of their estimates to generate consistent and reliable results.

OBJECTIVE OF THE STUDY

This thesis will develop a method of using remote sensing drones to capture 3D volume models of chip piles. Then by applying a conversion formula, that incorporates varying bulk density values, moisture content, and compression factors, to estimate the mass of the wood fibre of chip piles from the 3D model. In addition, this thesis will also examine the accuracy and precision of such a method, and attempt to improve on accuracies currently obtained by present mill estimation methods.

A SYNOPSIS OF THE STAGES IN THIS STUDY

This study uses aerial photography from unmanned aerial vehicles (UAVs), commonly known as drones to survey chip piles. This method's relevance increased due to the easy accessibility and lowering cost of UAVs and digital camera technology. Using drones and digital technology also allows for automation of a previously manual system thereby improving both the precision and accuracy of the mass estimations while reducing the cost of each survey. More importantly, there is a minimization in the risk to the survey crews, and maximization in the time reduction of the intensive methods previously employed to complete an inventory estimate. UAVs capture multi-view stereo images of the wood chip piles, which are then converted into three-dimensional (3D) digital representations of the piles using specific image analysis software.

Once in the 3D form, the volume of the pile is measured from the computer model and, through the application of calibrated formulas, the pile's value is converted into an accurate and reliable mass estimate.

This methodology can be simplified into five stages. The first stage is to capture imagery of the pile. In the second stage, software changes the imagery into a 3D digital model of the pile. The model is then measured for total volume, in the third stage, which is modified, in the fourth stage, based on compression factors of the shape and size of the pile. Finally, the fifth stage converts the compensated volume to a mass estimate using a specialized formula.

While specific models of UAVs and software packages, listed in this research and are capable of generating the 3D models desired for volume measurements, they are not the only ones capable of capturing and producing the necessary data. There are different models of UAVs, cameras, and 3D modeling software capable of generating similar results. The ultimate choice of which combination of equipment and software works best for the end-user should be based on specific project needs and budget limitations. For the purposes of this thesis, the focus of the research was to accomplish the survey process, to create the digital 3D image, and to understand when and where methods to improve accuracy and precision may be deployed to produce the best mass estimates.

The first stage of this analytical technique involves the use of UAVs, or drones, to acquire the aerial imagery used to generate the computer model. Capturing the imagery is performed using UAVs with on-board cameras. The two UAVs used for this analysis were the DJI Phantom 2 and the DJI Inspire. These drones are agile, highly responsive, capable of multiple types of flight modes, and come with built-in cameras. The camera is mounted to the drone with a 3-axis gimbal, ensuring the camera remains level in all flight conditions and the camera has a 94° field of view, which minimizes distortion. The UAV is flown over the wood chip pile and its surrounding area in a grid pattern. While the UAV is in flight, the on board camera automatically takes images of the ground in one of two ways. The first method is to have the camera triggered to take images at regular intervals and the second is to have the camera capture the whole flight in a video format where individual frames can be extracted back in the lab for processing.

In the second stage, the still images produced from the UAV's flight are analysed by 3D modeling software such as PhotoModeler-Scanner, AgiSoft's PhotoScan, or Pix4D-Mapper to create an accurate 3D digital model of the wood chip pile.

The third stage translates the 3D digital model into a volume measurement of the wood chip piles. The volume calculation, based on the 3D

digital model, is integral to the next step in the process: a step that varies greatly from current industry methods.

Once the third stage has successfully calculated the volume of the pile from the 3D images, the fourth stage converts the volume measurement into an accurate mass estimate. It is at this stage that the study varies from current methods of mass estimation. Once the height, shape, and size of each pile are determined, a formula is required to convert the volume to a mass estimate. Based upon discussions with mill supervisors, the formulas currently in use by industry are modified versions of a physics density formula that calculates mass from knowing volume and bulk density. These conversion formulas are usually historical averages incorporated into a density conversion formula. They are proprietary formulas developed by the mills, and are usually not in any academic publications. In this thesis, these mill conversion formulas will be grouped together using the term, Basic Linear Conversion (BLC) formulas. This is a term created by the author for ease of referencing and discussion. In a BLC method, the mass is estimated using a correlation between the volume of the chip pile and a single bulk density measurement of the wood chips. Depending on the company, the formula is usually modified by correction factors that are historically averaged calibrated variables. These correction factors came into being, through the mills' trial and error and pile calibration tests over many years of operation. Therefore, mills tend to keep these details as closely guarded secrets. This thesis develops a conversion formula that is accurate and

independent of the mill formulas and historical data developed by industry over the years.

Stage four, applies the assumption that bulk density is not a fixed value within a chip pile, and therefore a single standard bulk density cannot be applied as an averaged value for all variations of pile shapes and sizes. This is because wood chips at the bottom of the pile are under greater compression forces than those chips at or near the surface of the pile. Being under greater pressures causes the wood chips to have smaller void spaces between chips, resulting in smaller overall volumes, and, by direct correlation, higher bulk densities. Therefore, depending on the shape and size of a pile there will be different percentages of wood chips that are under high and low compressive forces, and a single averaged bulk density cannot account for all variations. Mapping and compensating for this varying bulk density in the chip pile allows for higher accuracy in mass prediction than using a single standard bulk density value for the conversion. Henceforth within this thesis, this estimation methodology using the variation in bulk density is referred to as the Compression Compensated Conversion (CCC) method. The CCC method is accomplished by the division of a chip pile into various smaller units of wood chips, which will be referred to as 'cells' of wood chips. This division will make it possible to determine the amount of volume loss due to compression on each cell. The volume loss due to compression is based on the amount of load from the column of wood chips above each cell. This means that even if two cells have identical volumes, the

cell that is subjected to greater compressive forces will contain a greater mass of wood fibre, as that cell will have a slightly higher bulk density than the other cells.

The fifth stage takes the compensation factor calculated in stage four and produces a mass estimate of the wood fibre available in the surveyed chip pile. This last stage is similar to the BLC method of mass estimation but it includes the compensation factor estimated by the CCC method. Overall, this compensation will improve estimates and reduce the differences between actual quantities of wood chips and inventory mass estimates of the chip piles in mill yards.

The industry is always interested in improving the accuracy of mass estimations, as errors in their chip inventory can add up to millions of dollars in discrepancies. In more extreme cases, these variations in estimates may lead to inefficient management practices for maintaining mill yard inventory, while regarded as necessary steps employed to overcome these discrepancies. For example, a mill may decide to maintain a larger stockpile to accommodate for the uncertainty in inventory quantities. The focus of this thesis explores the development of a practical application of the hypothesised CCC method in mill yards, while also identifying other possible areas of error that can further improve the accuracy of wood chip inventory in mill yards.

LITERATURE REVIEW

VOLUME CAPTURE USING STEREO IMAGERY ANALYSIS SOFTWARE

Walford (2009) describes a new technique capable of remotely capturing highly accurate 3D shapes of large outdoor features. By acquiring multi-view stereo imagery of the feature, it is possible to capture the shape and generate a 3D point cloud model in a computer. In the report, there is an example of a large gravel pile, complete with width, length, and height, captured in a 3D computer model using aerial photography (Walford 2009). This method can easily be applied to capturing the shape of a wood chip pile in a computer 3D model. These 3D point clouds generated can have accuracies that are comparable to point clouds generated by LiDAR systems (Strecha, et al. 2008), and are easier to acquire especially for reproducing larger outdoor features. Another report produced by EOS Systems Inc. (2012) suggests that their proprietary software PhotoModeler Scanner is not only capable of generating point clouds from multi-view stereo imagery, but the models generated can be as accurate as 1:44,000 when imagery is captured with an artificial planar scene where all parameters of the camera are known. More commonly, this ratio drops to about 1:9,000 in smart mode, which automatically analyses the images and allows the software to estimate all the details of camera parameters, position, and angles. In most cases, the point cloud generated has an error of $\pm 0.9\text{mm}$ at a 3.5-meter range from the object (EOS Systems Inc. 2012). It is due to this degree of accuracy

that this software is chosen for this study. The primary issue with this method of surface capture is the large point clouds generated to maintain a high degree of accuracy. These large data sets require a powerful computer to handle the analysis without resorting to excessive processing times. Researchers studying this issue have looked at algorithms, which can process these large quantities of data to reconstruct the surface without heavy memory use or long computer processing times (Hudson 2003). While these algorithms can optimize the data analysis, these techniques cannot be manually incorporated into existing software such as PhotoModeler Scanner. They use their own algorithms, but one can hope that regular updates by the company are incorporating new optimization techniques into their code. As an additional note, this technique of generating point clouds of large outdoor piles of biomass is already being studied by other researchers. A study by Trofymow, et al. (2014) looked at using remote sensing to capture volumes of burn piles in harvest operations. They have reported an improvement in estimations using remote sensing techniques compared to ground measurement methods, but they also stated there is room for improvement.

GLOBAL POSITIONAL SYSTEM (GPS) LOCATION CAPTURE ACCURACY

The capability to capture the features of a chip pile into a computer model is moot if the model does not match the real life chip pile. Therefore, it is necessary to review possible accuracy issues that may factor into this method of

volume capture. The techniques most commonly used in remote sensing systems are reliant on commercially available GPS units to determine the location and scale of the chip pile. If the scale of the model and image coordinates captured by the drone are being mapped using a commercial, on board GPS unit then coordinate accuracy is critical to determining the size of the error a GPS unit may impart to the chip mass estimates. For years, GPS units have been employed to record location of objects, and several studies have looked into the reliability and accuracy of these units to capture coordinates and trajectories. It is widely accepted that commercial GPS units can acquire stationary accuracies to within ten to fifteen meters and with additional systems enabled such as WAAS, it can improve accuracy down to a range of three to five meters. These positional accuracies were collected using averaged readings over a period of 30-minute intervals (Arnold and Zandbergen 2011). In another study, GPS accuracy was measured on a cyclist in motion. It was discovered that a GPS unit can achieve a mean absolute deviation of straight-line trajectories of 0.78 meters for non-WAAS units, and that deviation improves to 0.11 meters for WAAS enabled GPS units (Witte and Wilson, 2005). The same research team also discovered that while manufacturers claim their GPS units are accurate to velocities of 0.1 or 0.2 m/s actual measurements suggest that less than half of the velocity data meets that accuracy. Actual measurements found that only 45% of the time is the speed accurate to within 0.2 m/s. If the error range is relaxed to 0.4 m/s, it will include an additional 19% of the velocity data recorded. They go on to discover that error in velocity data

increases as the path changes from linear to circular due to a tendency to underestimate the travel speeds (Witte and Wilson, 2004). In another study, it was shown that GPS accuracy could change due to surrounding cover. Accuracy can change from an average of five meters from true position in an open sky setting, to ten meters under a closed canopy forest (Wing et al. 2005). What all these studies suggest is that the precision of GPS units vary from day-to-day depending on satellite visibility, obstacles that interfere with GPS signals and whether the GPS unit is in motion. This information suggests that while coordinates of GPS units can be very accurate, the precision can be compromised depending on conditions at that location when that coordinate is collected. It raises a concern for the accuracy of the scales created using GPS units, since the GPS coordinates are obtained while the image capture drone is in motion. In addition, there can also be interference due to buildings and silos in mill yards, which can block or bounce GPS signals. The smallest positional error in most cases still generates at least ten centimeters of uncertainty from any commercial GPS unit. Hence, care needs to be taken to minimize or eliminate these errors from affecting the final mass estimate of the chip pile.

COMPRESSION FORCE DISTRIBUTION IN PILES OF PARTICLES

Once volume of the chip pile is measured, there is a need to compensate for the compressive forces affecting the chip pile due to its shape and size. To be able to map these forces, it is important to understand how forces are

distributed throughout a chip pile. In physics research there have been studies examining and modeling the force transfers between particles in a pile. In most cases, the models predict the forces travel downwards with a bit of sideways deflection of forces in the outer layers of these piles. Based on these models, it is possible to predict and model the magnitude of the forces at any location in a pile (Oron and Herrmann 1998). This understanding does not mean that all piles will behave similarly. There is evidence that certain piles will exhibit non-uniformly distributed forces. Some piles seem to present a reduction in the downward force directly below the highest portion of the pile where it is expected to be the highest due to the amount of material in that area. While this phenomenon has been noted by several physicists, the reason for this dip in force under the peak is not well understood. Different studies have found variant conditions where such a dip in force is detected. One team found the condition occurred when the conical pile consisted of small particles like sand or very small glass beads, and as the particles got larger, the dip effect disappears (Brockbank and Huntley 1997). Another team noticed the reduction in the normal forces under the peak occurred when different sized particles in a pile were deposit into different conical layers. However, they noted that piles with different particle sizes that are not separated into distinct layers, but have the particles of different sizes randomly distributed in the pile would not generate a dip in the downward force under the peak (Liffman, et al. 2001). Considering that a wood chip pile is not composed of primarily small grain like particles, and the chips are not sorted in layers based on particle sizes, this phenomenon will

not be a consideration. It may apply to other studies when the pile consists of other biomaterials such as sawdust, which has smaller particles, but for the profile of sizes found in wood chip piles, the reduction of the normal force under the peak is not an issue. So the normal downward distribution of the forces can be used to model the forces in a chip pile.

LOSS OF WOOD FIBRE DURING STORAGE IN MILL YARDS

Another issue to consider when determining accuracy for mass estimation is the deterioration of wood chips that can alter the conversion ratio from volume to mass in a wood chip pile. Scientists initially studied this concern over 50 years ago. One study showed that deterioration occurs mostly in the outer layers of the chip piles, which had higher moisture content than the inner layers (Lindgren and Eslyn 1961). Of the different species studied softwoods like pine were revealed to deteriorate less vigorously as chips compared to when the pine is in rough pulpwood form. The primary concern of chip deterioration is micro fungi, which produces soft-rot in chip piles. This decay reduces the density of the pulpwood. While the rate of decay is not linear, it can be roughly estimated as about 1% to 2% loss per month during the warmer months of the year, and over a full year, the loss can be approximately 11% to 15% of its specific gravity (Lindgren and Eslyn 1961). The aforementioned research supports the premise that compensation of all the issues of wood chip deterioration can be monitored and compensated by the bulk density values of

the wood chips. Therefore, it is not required to calculate and compensate for this aspect directly.

ECONOMIC IMPACTS OF INVENTORY MANAGEMENT IN MILL YARDS

The focus of this study is to improve the accuracy of managing the wood chip inventory in mill yards. Supervisors at various mills suggest there can be discrepancies of about 10% between the different methods of estimating the mass of wood chips in mill yards. To see how much of an influence this discrepancy can affect the industry, a study that documented a paper mill's finances was used to put these discrepancies into perspective. Based on a case study about application of environmental management accounting at a Canadian paper mill, certain values and facts can be extracted. It disclosed that a mill's yearly wood chip supply could account for about 44.7% of a mill's yearly variable cost. This percentage can be in the range of \$20.7 million dollars (Gale 2006), which would mean a 10% variation in inventory could result in millions of dollars of which the financial department cannot accurately account. Since this variation in inventory changes depending if the mill had a small, medium, or large wood chip storage piles, it makes it difficult to control or compensate for these inaccuracies of inventory. Hence, minimizing these discrepancies is a critical issue to be addressed by the industry.

METHODOLOGY

As stated in the introduction, the ability to estimate the mass of the wood fibre requires multiple stages. These stages can be broken down to collecting multiple images of the pile, converting the images to a 3D model, segmenting the model into smaller cells of wood chips. Once the model is segmented into smaller cells, the CCC method can be applied. The CCC method determines a percentage to increase the volume of each cell to compensate for compression forces, and applies the bulk density to the modified volume to get the estimated mass of the wood chips in the pile. It was determined that to understand the factors which may affect the CCC method and its accuracy, data needed to be collected about volume measurement error, mass estimation error, 3D software modeling error, and technician error. All this would lead to the comparison of the CCC method with existing industry mass estimations to see what affects the new conversion method will bring to the accuracy of mass estimations in the mill yards.

PHASE I (DEVELOPMENT OF THE COMPRESSION CURVE)

In phase I, experiments were developed to explore the speed and magnitude at which wood chips compress, and decompress depending on the compression pressures applied to the wood chips. This exploration was accomplished in three parts to identify three factors of volume changes. The

three factors are initial compression, sustained compression, and decompression behaviour on the volume of wood chips. Initial compression measures the volume change immediately after force is applied to a wood chip pile. Sustained compression measures volume changes after a mass has been loaded on the chip pile and it has been given time to settle. This settling allows chips to shift over time and reduces the void spaces between chips to a minimum under sustained load forces. The third part looked at decompression of the wood chips after a sustained load is removed from the pile, and the chips have time to decompress from the removal of the compressive force. All three parts were measured using the same experiment parameters. These parameters consisted of a system of compressing and decompressing wood chips in a barrel by applying heavy barbell plates onto the wood chips and recording changes of volume over time. The weights or load plates used to generate a compressive force are the same as barbell plates used by weight lifters at the gym.

Figure 1 below shows the experiment setup. A hard plastic 44-imperial gallon drum is loosely filled with varying volumes of wood chips. Next, a levelling plate with a mass of about 4 kg is used as a cap at the top of the wood chips to ensure it is level, and to ensure even distribution of force over the whole top of the wood chips when the weights are loaded into place. Each load plate has been premeasured and the exact mass is determined and labeled on each plate. The volume of wood chips is measured by calculating the distance

between the levelling plate and the lip of the barrel in the four cardinal directions. This ensures the plate is level, and, in conjunction with the known dimensions of the barrel, it gives enough information to calculate the volume of the uncompressed wood chips loaded into the barrel. An initial measure of distance from the center mark on the levelling plate to the bottom edge of the measurement bar placed over all the barrels is taken to define the initial condition. Next, a predetermined mass is placed on the levelling plate and the distance to the measurement bar is immediately noted. Then, without increasing the load, the distance is measured over the day at intervals of one minute, five minutes, fifteen minutes, thirty minutes, one hour, two hours, eight hours and twenty-four hours. After a day under a compression load, the load plates are removed and the displacement distance from the levelling plate to the measurement bar is, once again, measured at one, five, ten, fifteen, twenty, thirty, forty-five, and sixty minutes. This second series of measurements are recorded to determine the decompression rate of wood chips after a compressive load is removed. The entire procedure is repeated using different volumes of wood chips, different compression load masses, and each configuration setup is replicated in three barrels to confirm no other variables are affecting the results. These values are then used to generate time compression and decompression curves. Results from these curves are used to determine some of the parameters in the next stage of the experiment.



Figure 1: Three 44-imperial gallon barrels used for compression and decompression testing.

To develop the maximum compression curve, the same equipment configuration as used in the previous stage is used, but this time only a single measurement is taken per compression load. The distance is measured at the eight-minute interval, followed by increasing the compression load and taking another reading after the next eight-minute interval. This process continued until the compression distance stops changing regardless of the increase in load mass placed onto the levelling plate. This methodology is used to determine the max compression achievable for that specific volume of wood chips. The point of this was to develop a curve that can predict the volume loss when a certain amount of compression force is placed on the wood chips. As with the previous

stage, this was repeated with different volumes of wood chips and each configuration was replicated in the three barrels. Once the compression curve was developed, it was possible to convert volumes to masses that were dependant on the compressive loads applied to the wood chips.

PHASE II (PROOF OF CONCEPT ON A SMALL SCALE)

Phase II was performed on a small pile of wood chips. The wood chips were measured in a one-cubic-meter High-Density Polyethylene (HDPE) liquid container, which was then lifted by an automobile engine hoist onto an industrial floor scale to determine its mass, as seen in Figure 2. The amount of chips is shown in Figure 3. The wood chips filled the container 100.8 times giving the pile a loose volume of 100.8 cubic meters and each time it was filled it was weighed, which had the combined total of 30,820 kg. In addition, the wood chips were processed using standard moisture content tests and sorted using a wood chip screener to determine chip size distribution. This information was recorded for control purposes and for comparison with mass estimates in the later phases.



Figure 2: One cubic meter container used for measuring the wood chips on a small scale pile.

Once the total mass and volume of the wood chips were determined, all the chips were manipulated into a cone like pile roughly 3.4 m tall, as shown in Figure 3. The chips were left alone for two days to settle and stabilize before any attempt to capture its shape and volume was made. The capturing of the shape and volume was accomplished using a digital camera and a tripod. Each set of pictures consisted of approximately 75 digital images, which were taken from all angles around the chip pile at a distance of 5 meters from the closest bottom edge of the pile, and at 1.6 m above ground level. This process is

described in detail later in this section. As the process took place in a large warehouse with artificial lighting of equal intensity at regular intervals, it ensured the photos around the pile had a uniform light exposure. Each set of photos consisted of a full 360° view of the chip pile and each photo was spaced evenly around the chip pile. Multiple sets of photos of the same chip pile were taken following the same procedure used for the first set of images. In total 15 sets of images were captured of the cone shaped pile.



Figure 3: Small-scale wood chip pile shaped into a conical shape.

The next stage of this phase involved reshaping the pile from its previous cone shape to a more flattened shape that was no higher than 1 meter at any point of the pile as seen in Figure 4. The conical pile was flattened by a bulldozer scooping the chips off the top of the pile and unloading it around sides of the chip pile. This new pile was allowed to decompress and equalize for two days. After the decompression, the flattened pile was photographed in the same fashion as that of the cone shaped pile. Images were captured approximately 5

meters away from the closest bottom edge of the pile and these sets required 100 equally spaced images to capture the 360° view of the pile due to the increased base diameter of the pile. Due to issues noticed in the 3D surface generation from the cone shaped pile, 18 sets of images were collected of the flattened pile, in order to replace any sets that generated poorly captured 3D surfaces with the reserve sets already collected on the same day.



Figure 4: Small-scale pile reshaped into a flattened pile.

Regardless of the pile shape, conical or flattened, each set of images was processed using the analysis software called PhotoModeler-Scanner. This software takes all of the images and calculates the location and angle of each photo based on different stereo pair images. This process can be seen in Figure 5, where the camera positions are defined by the blue boxes and the direction of the lens is indicated by the green cylinders. After determining the position of the camera for each photo, it looks at each image and using the different angles of the camera it can triangulate the X, Y, Z position of the pixels or patterns it finds

in common between photos. When enough of these pixel positions are determined, it connects them to form a surface of the object in the virtual 3D computer model. Next, this model can be scaled properly using known control points and distances so that the size of the model can be determined. In Figure 5, the line across the pile is a measured control distance introduced for scale purposes. This generates a 3D model of the chip pile that can be manipulated and the volumes can be estimated with a high degree of accuracy.

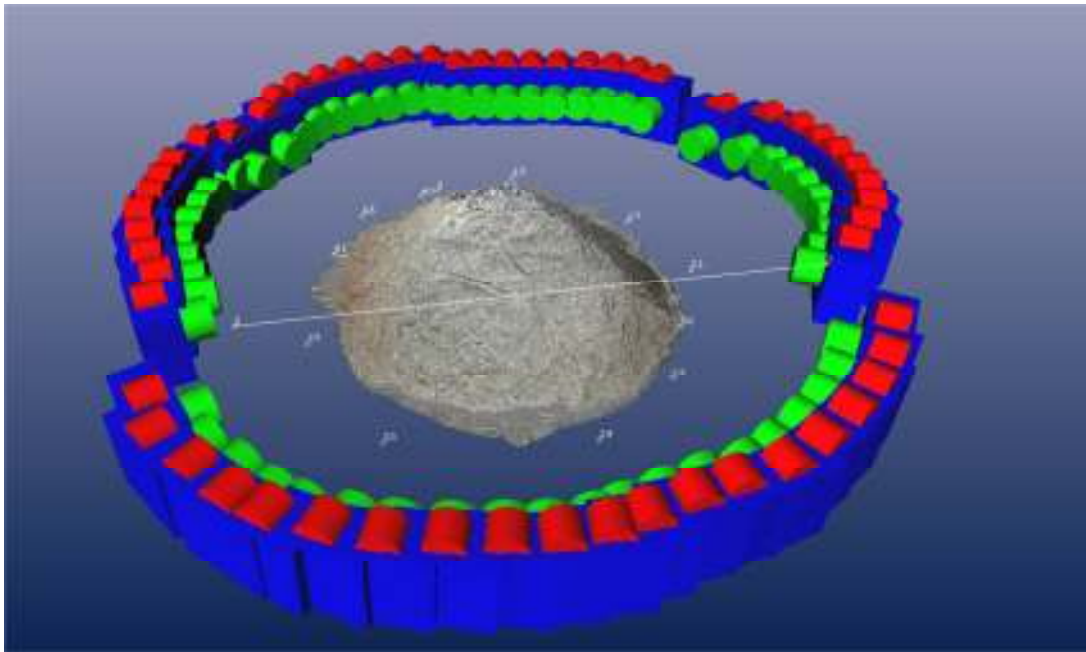


Figure 5: 3D model of the chip pile showing the location of all the camera locations.

This process was repeated for each image set captured for both the conical and flattened piles. The best 10 sets of the conical and the flattened piles were used to calculate the volumes of the chip pile. Models with voids in the surfaces were not used, as the void areas required the software to make an estimation of the missing surface areas, which may be incorrect hence, the

collection of more than 10 sets per pile shape. Figure 6, shows an example of both the conical and the flattened pile converted into 3D computer models.



Figure 6: Transition from photo image to 3D model on the computer for both conical and flattened piles.

To estimate the mass of the wood chips, the shape of the pile is segmented into multiple layer slices. Each layer is compensated for volume loss due to compression from the mass of the chips piled above that layer. This is determined based on the compression curve developed in phase I. All the compensated volumes are then summed up to generate a new uncompressed total volume and when multiplied by the bulk density gives an estimated mass of the pile. All these calculations were performed in an excel spreadsheet. These estimated masses are then compared to the manually measured total mass of

the chip pile. The accuracy of this method is determined through a comparison to the measured mass of the whole pile.

PHASE III (MEDIUM SCALE ANALYSIS)

After developing the method to estimate the mass of wood fibre accurately from chip pile imagery, it was important to field test at mill sites. The first test site was at a mill located in Longlac, Ontario. This chip pile at this site was tested using the method developed in the small scale warehouse testing. Figure 7 displays an aerial view of the chip pile in Longlac. The first step was to take radial positioned photographs around the chip pile. This pile required over 200 images to cover the whole pile radially, standing about 10 to 20 meters from the base of the pile. To test an additional method, an aerial video was taken of the whole pile using a DJI Phantom 2 drone. By extracting frames from this video, it was possible to create a second set of imagery comprised of roughly 140 images of the chip pile using a top down view. For these sets, both radial and aerial images were processed as described in Phase II using the PhotoModeler-Scanner software to generate a 3D model of the chip pile. Based on the results from this test, it was determined aerial photography required fewer images to generate a cleaner model that did not contain voids.



Figure 7: Aerial view of the chip pile at the mill in Longlac taken using a Phantom II - DJI drone.

To test if it was possible to improve accuracy without having to fly multiple missions over the same pile, the 140 images were randomly sorted out into multiple sets. By randomly selecting roughly 100 images evenly distributed from the full set of 140 images, it was possible to create multiple image sets. This technique was used to generate multiple 3D models of the pile with the primary objective to test volume measurement accuracy. For example set one may include images 1,3,4,7,8...138, set two may include images 2,3,5,8,9...140 and set three may include 2,3,6,7,9...139 etc. The images have a high percentage of overlap between images. This overlap ensures that eliminating some of the images from the full set will still leave a subset of images that has full coverage of the entire chip pile. This method of generating subsets from one UAV flight will be explained in detail in the error portion of the discussion section of this thesis.

Based on the results at Longlac, an arrangement with a mill in Thunder Bay permitted the survey of three chip piles for five consecutive days. See Figure 8 for a sample overhead view of the chip piles at the Thunder Bay mill. Comparing the estimated results with the mass values provided by the mill themselves allowed the test of the CCC method on a larger scale. The three piles of wood chips changed volumes on a daily basis throughout the week, and comparison of mill and CCC mass estimates on a daily basis allowed accuracy analysis of the new method. Each day at a known time, an aerial survey was taken of the chip piles. By knowing the exact time the aerial photos were taken it was possible to determine the quantity of wood chips on the pile by calculating which truck loads were already delivered to the chip pad at the time of the survey. Using the techniques developed over the previous phases, each pile on each day is calculated by averaging three sets of images. These values were then compared to the values supplied by the mill to check for accuracy. The conversion used the compression curves developed in phase I, and the bulk density used in the formula followed ASTM standards for measuring bulk density (ASTM International 2016). It was not feasible to generate a bulk density as in phase II where the whole pile was measured for its mass and uncompressed volume.



Figure 8: Overhead Drone Photo of the chip pile in Thunder Bay.

PHASE IV (ERROR ANALYSIS AND LARGE SCALE PREDICTIONS)

At the end of Phase III, it was noticed that the system was accurate but there were still some error discrepancies compared to figures delivered by the mill. To improve the accuracy phase IV analysed where the errors were being generated and looked at how to reduce these errors.

In phase II, it was noticed that by averaging multiple sets of images it was possible to improve the precision of the estimations. To examine the benefits of adding this step into the process, a 10,000 iteration Monte Carlo simulation was applied to analyse both conical and flattened shaped piles from phase II. The simulation utilized the normal distribution curve of the values from the ten estimated mass calculations to generate new estimates. For each shaped pile, three cases were generated. Case 1 simulated 10,000 estimates without the use of averaging. Case 2 simulated 10,000 estimates using an average of five image sets for each mass calculation. Case 3 simulated 10,000 estimates using an average of ten image sets for each mass calculation. The three cases were generated for both the conical and the flattened piles and then the basic statistics of each case was reviewed to determine the effectiveness of applying the averaging method into the mass estimation.

Part of the error was determined to come from technician or operator accuracy. When the imagery is processed by PhotoModeler-Scanner, the

control points that define the scale have a source of human input error, which is introduced into the scale of the model. These control points will shift slightly depending on where the technician identifies the control points are in the images. To examine this error, multiple processing runs of the same image set were performed. Each run required the technician to identify the control points as they normally would. With all other variables the same, the results from all the runs were analysed to see what percentage of the final error is attributed to the technician due to the need to identify control points in the images. It was possible to attribute the error to the technician since the image set and the software used were the same every time. The only place an error can be introduced is by the operator identifying the location of the control points.

Another part in the process where error could occur is from the choice of software used to generate the 3D models. Different software uses different algorithms to estimate the location of the surfaces. So to see how much this contributes to the total error, the same image sets were processed using two different software packages. In phase III, the image sets used for estimating chip piles at the mill were processed through AgiSoft's PhotoScan and PhotoModeler-Scanner. The volume results from both software packages were compared with each other and the differences were analysed to determine the portion of the error that is contributed by the software algorithms.

Finally, it was necessary to examine how volume to mass conversions can vary depending on the scale of the chip pile. The same 3D model was processed through the CCC method and a simplified mill conversion formula. This was repeated when the pile had its xyz dimensions increased by three times, and it was repeated again with the xyz dimensions increased by ten times the original size. The differences between methods were compared to see if the scale altered the magnitude of difference between the two methods.

RESULTS

COMPRESSION, DECOMPRESSION, AND TIME COMPRESSION CURVES

In Phase I of this project, the physical characteristics of the supplied wood chips were analysed to gather the behaviour of the chips under physical pressures. The first experiment was designed to examine how the volume changes over time as a force is applied on a volume of wood chips. The results are shown in Figure 9 were based on various static loads that were applied to the chip piles. Each time a load was applied, the effects were monitored for over 24 hours, but only the first 3 hours is graphed, because after 3 hours all the piles had reached a steady state. The y-axis displays the amount of volume loss, based on a scale where 0% is an uncompressed pile and 100% is a pile that has reached maximum compression for the load placed on the chips. Notice that at least 60% of the volume loss happens at time zero, and in some cases, the pile reaches 100% volume loss immediately after applying the load. In most cases, the compression has passed the 90% mark by the one-hour interval.

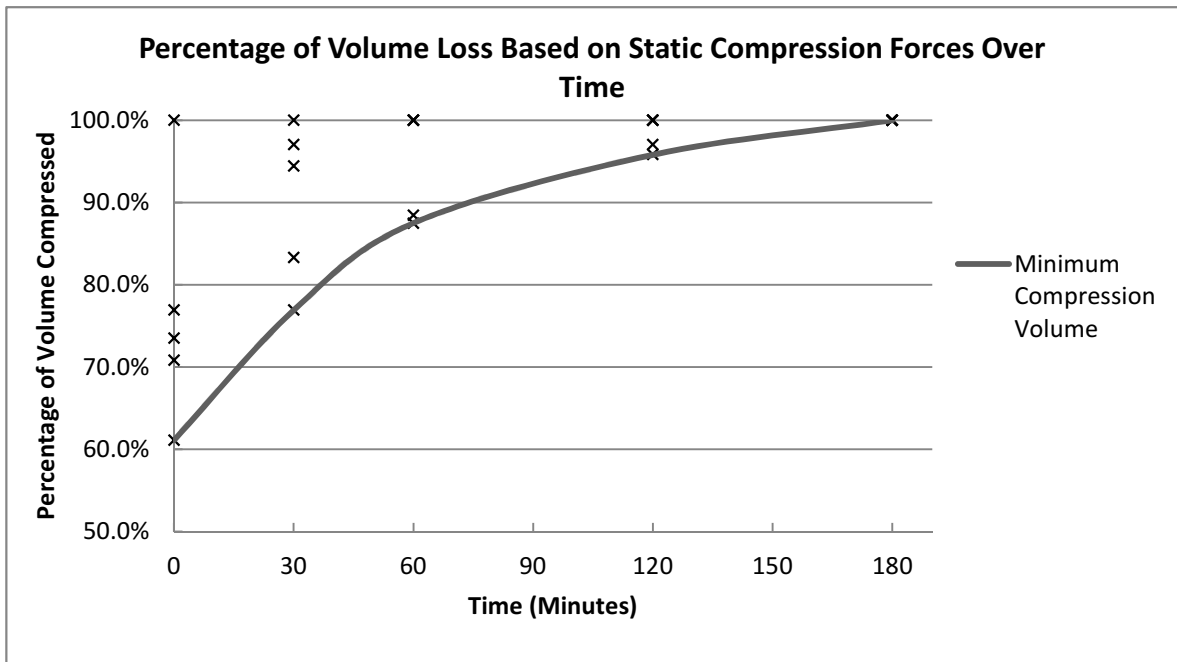


Figure 9: Graph showing the percentage of volume loss due to static compression applied over time.

The next physical response to be examined was how the chips decompressed after the load was removed from the pile. The results for this portion of the experiment are not as definitive as the time compression graph. The data points are scattered between the maximum and minimum boundaries (Figure 10). The chip piles immediately recover a third of the compressed volume loss and will eventually recover as much as 57% of the original volume loss after 30 minutes. The piles were left for at least 24 hours to see if they would decompress further, but no further decompression occurred after the 30-minute interval without physically shaking the barrel and manually stirring and loosening the wood chips. If the chips are manually decompressed, it will return to the original state with 100% volume loss recovered. Overall, the decompression is not consistent, as barrels of chips seem to recover a random

amount of lost volume limited between the boundaries (see Figure 10). The reason one pile would recover a third and another pile would recover half the original lost volume during decompression is not clear, however some suggestions will be made in the discussion.

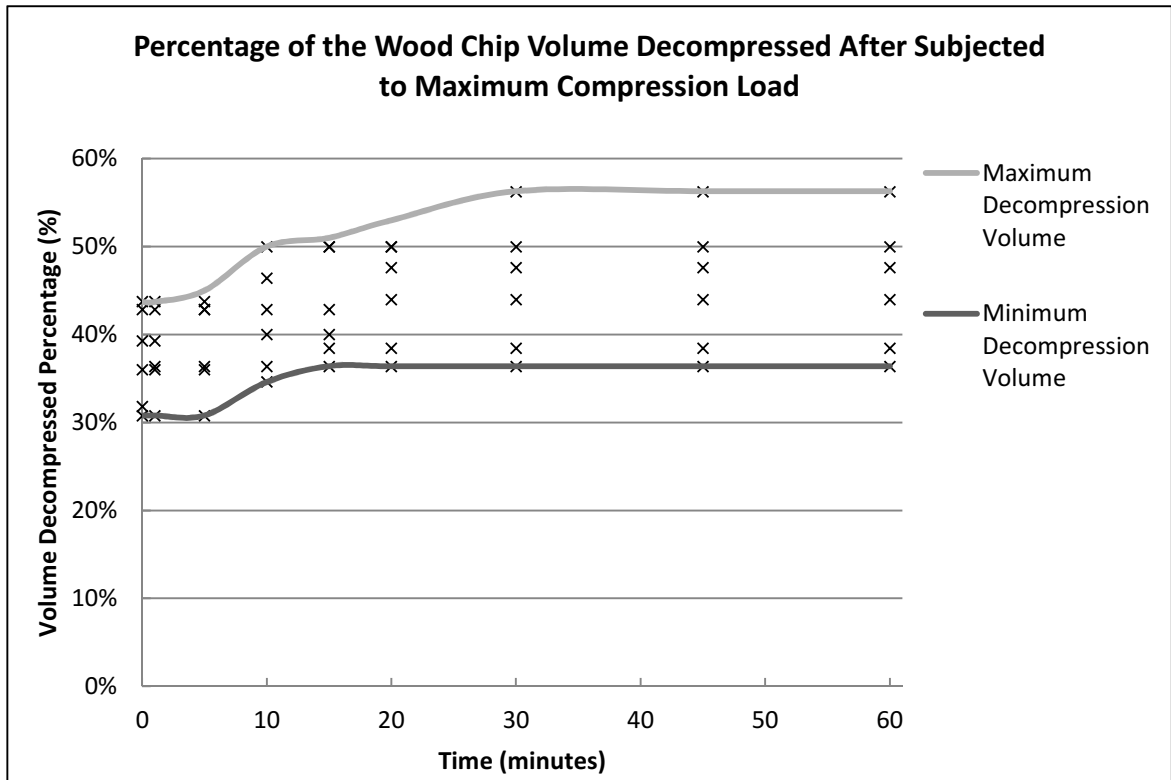


Figure 10: Graph showing the range of wood chip decompression over time.

The next experiment looked at the percentage of volume loss based on the pressure applied to the top of the chip pile. Multiple runs with various loads and volumes were processed and all plotted on the same graph shown in Figure 11. Every run appeared to follow a similar curve, and when plotted together it was possible to generate a trend line that predicts the change of volume based on applied surface pressure with a R^2 value of 0.96 (see Figure 11).

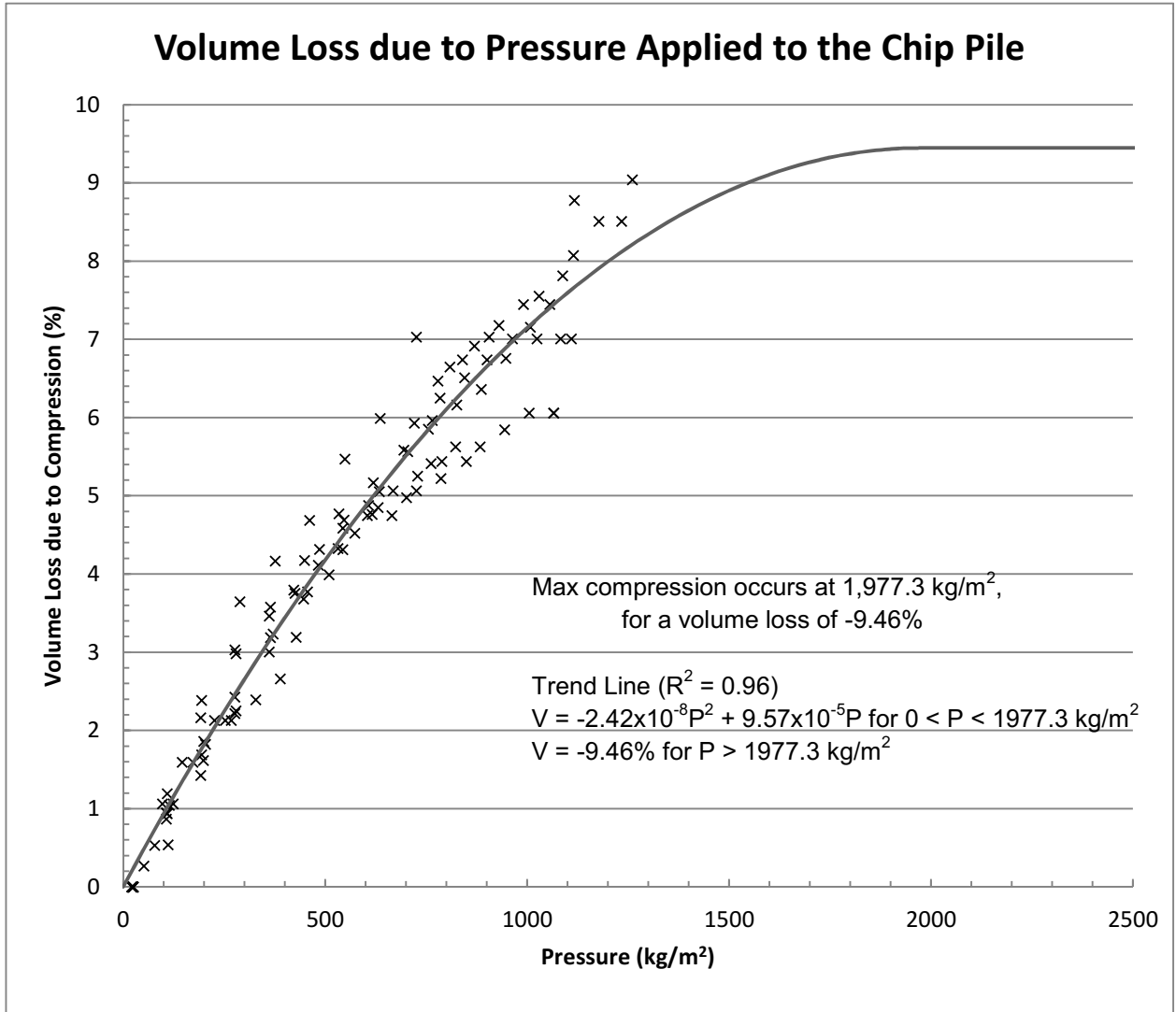


Figure 11: Chart showing the volume loss due to pressure applied on to the wood chips.

The trend line formula is listed below as Equation 1. It is used to predict the volume loss (V), when the pressure (P) is entered into the equation. The equation of the trend line is actually a parabola and will eventually curve back down at around 1977.3 kg/m^2 . Since the volume will never start to decompress while increasing the applied pressures past the limit of the curve, the second

half of the trend line is converted to a flat line, indicating the maximum compression has been reached. This asymptotical curve matches the individual compression curves seen in each individual repetition of this experiment. To determine this limit, the derivative of Equation 1 is taken and V' is set to zero to determine the pressure at maximum compression. This is shown as Equation 2. It is determined that 1977.3 kg/m^2 is the minimum pressure to achieve maximum compression, and when this pressure is substituted back into Equation 1, the maximum compression for these chips is determined to be at 9.46% volume loss.

$$V = (-2.42 \times 10^{-8}) P^2 + (9.57 \times 10^{-5}) P \quad \text{Equation 1}$$

$$V' = (-4.84 \times 10^{-8}) P + (9.57 \times 10^{-5}) \quad \text{Equation 2}$$

SMALL SCALE CHIP PILE VOLUMETRIC AND MASS ESTIMATIONS

To have an accurate value to judge the accuracy of the estimates generated by the different methods, the chip pile had to be measured manually. The chip pile was measured one container load at a time and was filled 101 times with the last load being only 80% full. This generated the measure volume of 100.8 m^3 with an error of $\pm 1.01 \text{ m}^3$. The masses summed up to 30,820 kg with an accumulated error of $\pm 5.02 \text{ kg}$ as the certified industrial scale used has an accuracy of $\pm 0.5 \text{ kg}$. Combining these two values generates a loose bulk density of about 305.8 kg/m^3 . It should be noted that this bulk density value is a calculated loose bulk density. After phase II, all bulk densities were determined

using an ASTM standard bulk density measurement, which is a more precise bulk density value than a loose bulk density calculation. The full reason will be explained later in the discussion section.

During phase II, the volume of the pile was calculated using PhotoModeler-Scanner and subsequently converted to the mass of the wood chips using the following conversion formulas.

$$M = V \times D \quad \{BLC \text{ Method}\} \quad \text{Equation 3}$$

$$M = (1+C) \times V \times D \quad \{CCC \text{ Method}\} \quad \text{Equation 4}$$

The BLC method listed above as Equation 3, provides an estimated mass using the volume (V) of the pile, and the bulk density (D) of the wood chips. The CCC method listed above as Equation 4, takes into account an extra compensation variable (C) which increased the volume by the estimated percentage for the volume loss due to compression. This will be explained in detail in the discussion section.

The first configuration of the wood chips was a conical shaped pile and using ten images sets, ten volumes were measured of the same pile. From the ten volumes, twenty mass estimates were generated which consisted of ten estimates using the BLC method and ten using the CCC method. All mass estimates were compared to the total chip mass previously measured using the HDPE container. Table 1 shows both methods produced estimates that have a

similar standard deviation spread with a range of about 18% difference between the maximum and minimum values. The only difference was that the CCC method had better averaged accuracy compared to the BLC method. The overall average mass of the CCC estimates was about 1.6% off from the manually measured mass whereas the BLC estimates average was about 7% off.

Table 1: Descriptive statistics for a small conical pile showing the difference between BLC and CCC conversion methods.

Cone Shaped Pile	Basic Linear Conversion (BLC)	Compression Compensated Conversion (CCC)
Measured Mass of Wood Chips	30820.0	30820.00
Average Estimated Mass	28572.9	30329.8
Percentage Difference	-7.29%	-1.59%
Standard Deviation	1532.2	1630.6
Maximum Estimate	1.6%	7.8%
Minimum Estimate	-15.9%	-10.8%

Similar results were noticed when estimating masses of the flattened chip pile (Table 2). This time there was a range of masses, which has about 14% difference between maximum and minimum estimates. The overall accuracy was about 4% less than the measured mass, but this time there is only a difference of about 2% between the two methods.

Table 2: Descriptive statistics for a small-flattened pile showing the difference between BLC and CCC conversion methods.

Flatten Pile	Basic Linear Conversion (BLC)	Compression Compensated Conversion (CCC)
Measured Mass of Wood Chips	30820.0	30820.0
Average Estimated Mass	29390.4	29786.3
Percentage Difference	-4.64%	-3.35%
Standard Deviation	1254.2	1282.8
Maximum Estimate	5.0%	6.5%
Minimum Estimate	-8.8%	-7.6%

To determine if the differences between the BLC and CCC methods were statistically significant, one-way anova analyses were applied to the conical and flattened pile cases. The results were different depending on the shape of the pile as hinted by the averages shown in Tables 1 and 2. Table 3 shows that when the chips were arranged in a conical chip pile, there was a statistically significant difference between the two methods, but for the case with the flattened chip pile, there was no statistically significant difference.

Table 3: Chart examining the F statistics and significance level of mass estimation between BLC and CCC conversion methods, for conical chip and flattened chip piles.

Pile Configuration	F statistic	Significance Level
Conical shaped pile	$F(1,18) = 6.166$	$p = 0.023$
Flatten shaped pile	$F(1,18) = 0.487$	$p = 0.494$

MEDIUM SCALE ANALYSIS

Aerial images were taken on consecutive days using a hex-copter drone with a downward pointing camera. The images captured three piles over five days. These piles grew and shrank daily with piles A and B being roughly conical and pile C being a flattened pile. Notice the images in Figure 12 to 15 showing the key days with transitional changes over the week. Pile A grew in size until Thursday of that week, at which point it was being consumed by the mill on Friday. Pile B had the opposite behaviour as it was consumed by Thursday where a new pile was being formed on Friday. Pile C being located

over the screws that draw the chips into the mill was being fed with chips and remained relatively consistent in size and shape throughout the week.



Figure 12: 3D model of the chip piles on Monday June 15.



Figure 13: 3D model of the chip piles on Tuesday June 16.

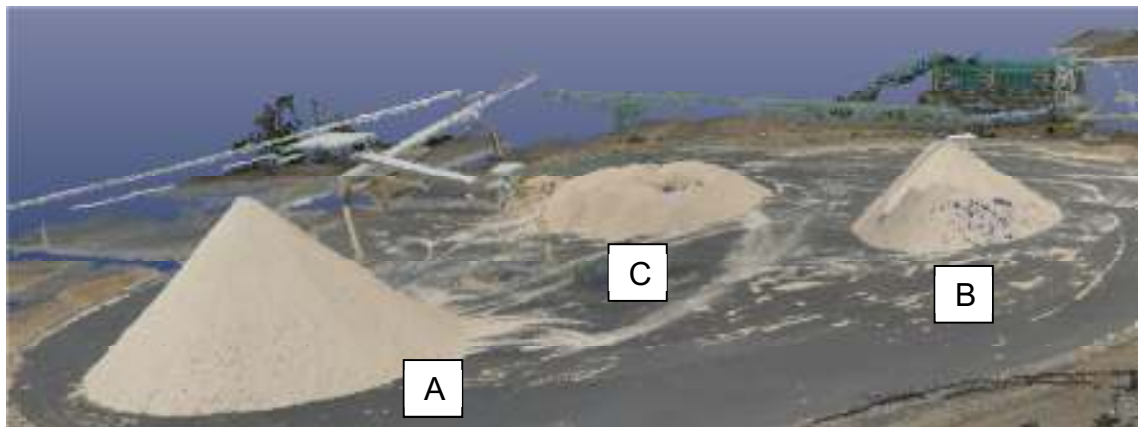


Figure 14: 3D model of the chip pile on Thursday June 18.



Figure 15: 3D model of the chip piles on Friday June 19.

Table 4 shows the difference between the mill's chip mass estimate and CCC method of estimating chip mass where the difference between the two methods varied by about 2.7%. It also confirms that the CCC method of estimation is accurate enough to track the variations of mass in each pile on a daily basis.

Table 4: Daily mass estimations of three chip piles at a local mill comparing the differences between CCC method and the mills method.

Date	Pile	Volume (m ³)	CCC Mass Estimate (t)	Mill Mass Estimate (t)	Difference (t)	Percentage
15-Jun-2015	A	7,961.9	1,425.3	1,386.9	-38.42	-2.70%
	B	2,425.6	430.1	422.5	-7.54	-1.75%
	C	2,666.5	465.8	464.5	-1.33	-0.29%
16-Jun-2015	A	5,121.1	912.7	892.0	-20.70	-2.27%
	B	5,012.3	894.2	873.1	-21.11	-2.36%
	C	2,895.6	505.6	504.4	-1.22	-0.24%
17-Jun-2015	A	2,125.7	375.1	370.3	-4.86	-1.29%
	B	8,262.2	1,475.1	1,439.2	-35.88	-2.43%
	C	2,321.5	404.6	404.4	-0.22	-0.05%
18-Jun-2015	A	2,257.0	397.3	393.2	-4.19	-1.06%
	B	9,226.2	1,652.8	1,607.1	-45.72	-2.77%
	C	2,465.9	429.5	429.5	0.03	0.01%
19-Jun-2015	A	4,945.0	880.4	861.4	-19.00	-2.16%
	B	4,715.6	838.9	821.4	-17.44	-2.08%
	C	2,811.6	490.2	489.8	-0.46	-0.09%

Through further sorting of the data in Table 4 certain trends are noted. Mill estimations of the oven dry mass in conical piles A and B were consistently less than values generated using the CCC method by about 2%. However, in the analysis of the flatten pile C both the mill's method and the CCC method only deviated from each other by about 0.13% over the whole week. This result is summarized in Table 5.

Table 5: Comparison of the mass estimates on Table 4 sorted and averaged based on the conical and flattened pile shapes.

Descriptive Statistics	Piles A & B	Pile C
Standard Deviation	0.56%	0.13%
Average	-2.09%	-0.13%
Minimum	-1.06%	0.01%
Maximum	-2.77%	-0.29%

PREDICTION OF COMPRESSION FORCE DISTRIBUTION IN A CHIP PILE WITH CROSS-SECTION MODELING

Based on the findings of the experiments the following compression properties and behaviours were deduced from results of Table 1, 2, 4, 5, and Figure 11. The cross-section models in Figures 16, 17, and 18, predict the force distribution within the piles by varying three distinct physical variables. In each pile, the cross-sections are broken down into multiple cubic units of wood chips or 'cells' of wood chips. For simplicity, each cell can be under the influence of light, medium, and heavy compressive forces depending on the number of cells above applying a compressive load. In the prediction models, the top cell in each column of wood chips is not subjected to any compressive forces from

above and is represented by the white cells, which have little to no loss of volume. The light grey cells represent on average 5% loss in volume and are under medium compression from the light cells above. The dark grey cells are wood chips that are subject to the heavy compressive forces from the light and medium cells above them. Each of these heavy compression cells are under max compression, and these cells will have a volume loss of 9.46%.

The three cases A, B, and C presented in Figure 16 all have a size of 16 cells stacked in different configurations. While their overall size is the same, they have different quantities of light, medium, and heavy cells. Figure 16, demonstrates the difference of compression forces based on the shape of the pile. Notice the piles vary from a flattened pile to a tall column of wood chips, such as in a wood chip silo. After analyzing the different compression distribution, A has an overall estimated loss of 6.0% in volume, B has a loss of 2.5% in volume, and C has a loss of 7.7%.

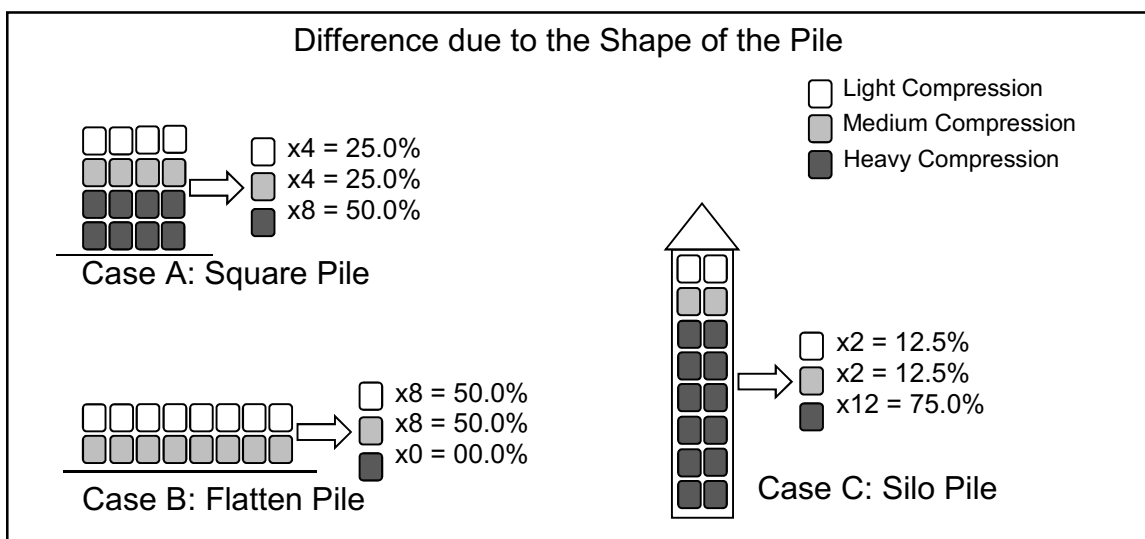


Figure 16: Showing the different varying densities of wood chips throughout a chip pile as shape varies from a square pile, a flattened pile, and a tall pile in a silo.

In Figure 17, case D and E show how the height of the pile changes the percentages of the various compression cells. In these models, case D is a third higher than case E with max compression reached at two cells deep. Once again, analyzing the compression of cells predict that D has a loss of 5.5% of volume, whereas E has a loss of 3.9% of volume.

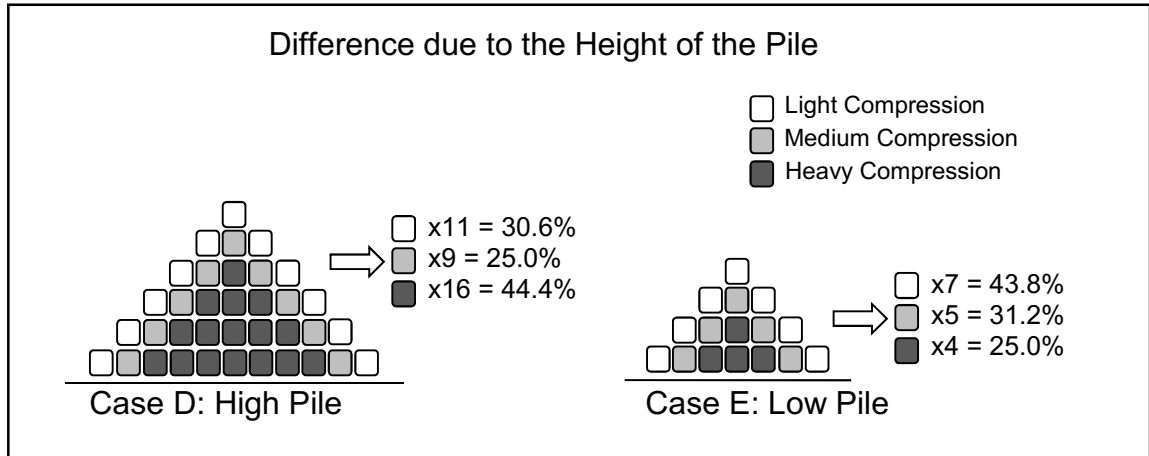


Figure 17: Showing the different varying densities of wood chips as the pile changes in height.

Figure 18 shows the difference between low-density wood chips and high-density wood chips. Both cases are the same size but pile F has a higher bulk density than pile G. Calculating the loss of volume due to compression, pile F shows a loss of 5.5% whereas pile G shows a loss of 2.7%.

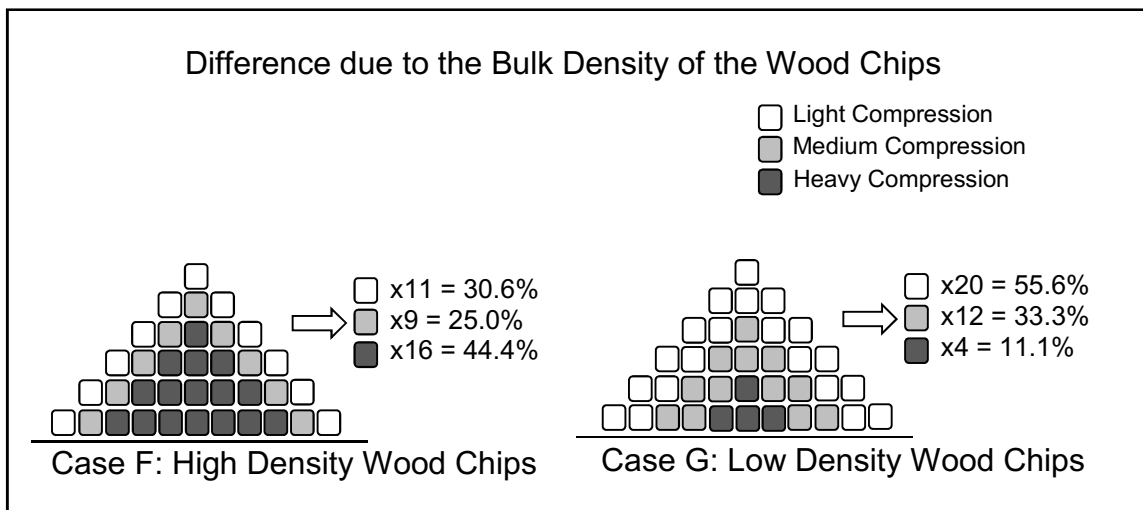


Figure 18: Showing the different varying densities of wood chips as the bulk density changes.

ERROR IDENTIFICATION AND REDUCTION ANALYSIS

Large Scale Skew

To examine if the relationship between volume and mass scaled equally as the volume of the chip pile is greatly increased, an exploratory analysis was performed using known formulas, and chip pile shapes from phase III. The 3D models of piles B and C were increased to twenty-seven and a thousand times its original volume. These scales were chosen based on increasing the XYZ axis of the model by three and ten times their original linear length. Pile B representing conical shaped piles and pile C representing flattened shaped piles. Using the CCC method and compensating for moisture content the oven dry wood fibre mass was estimated. This mass estimation is compared with values obtained by applying the mill formula for the same enlarged volumes. The results shown in Table 6, match the results in Table 5 with the original scale being within 1.8% of each other. When the volume increases by factors of 27 and 1000 the two methods begin to deviate in mass estimates. When all the models were processed, the estimated oven dry mass of the chips ranged from 3.5% to 5.6% between the two methods.

Table 6: Chart showing the difference between CCC and mill estimates for both conical and flattened pile shapes when increasing the size of the pile by factors of 27 and 1000.

Shape and Scale	Volume (m ³)	CCC Mass Estimate (t)	Mill Mass Estimate (t)	Difference (t)	Percentage
Conical Volume x1	2,425.6	430.1	422.5	-7.5	-1.75%
Conical Volume x27	65,490.3	11,929.5	11,407.8	-521.7	-4.37%
Conical Volume x1000	2,425,565.0	447,464.0	422,511.2	-24,952.8	-5.58%
Flattened Volume x1	2,666.5	465.8	464.5	-1.3	-0.29%
Flattened Volume x27	71,994.3	12,992.4	12,540.7	-451.6	-3.48%
Flattened Volume x1000	2,666,455.7	489,515.6	464,472.2	-25,043.5	-5.12%

The examples from Table 6 are modeled in a graphical view mapping the compression within the piles (See Figures 19 and 20). The compression distributions for both conical and flattened piles, labeled as Case I and L have minimal heavy compression volumes for the piles measured in the mill yard, but when the volumes were increased by 27 or 1000 times the original size, the percentage of volume under heavy compression greatly increased to over 50% of each pile.

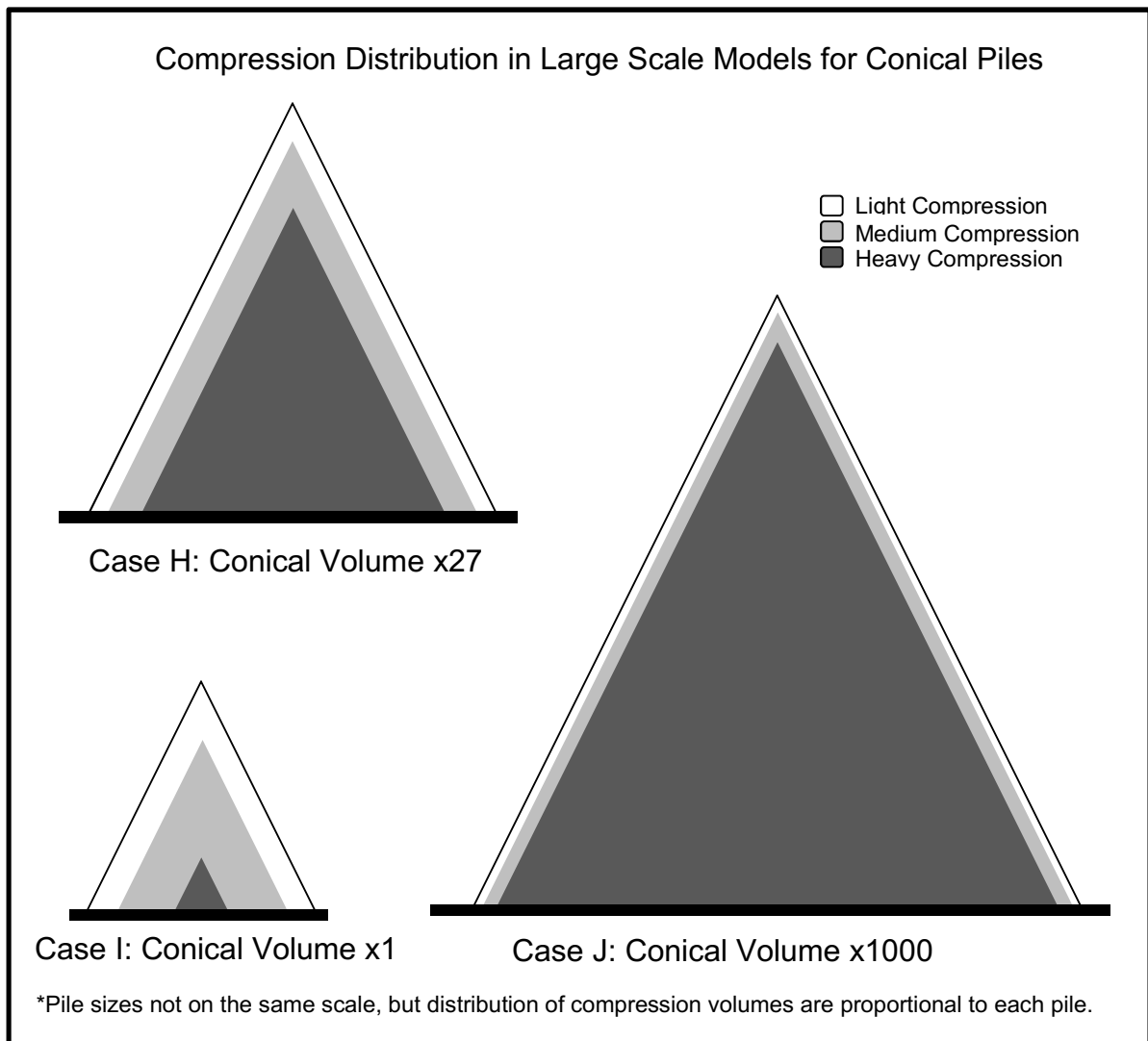


Figure 19: Graphic models of compression distribution in the predicted conical piles of Table 6: Chart showing the difference between CCC and mill estimates for both conical and flattened pile

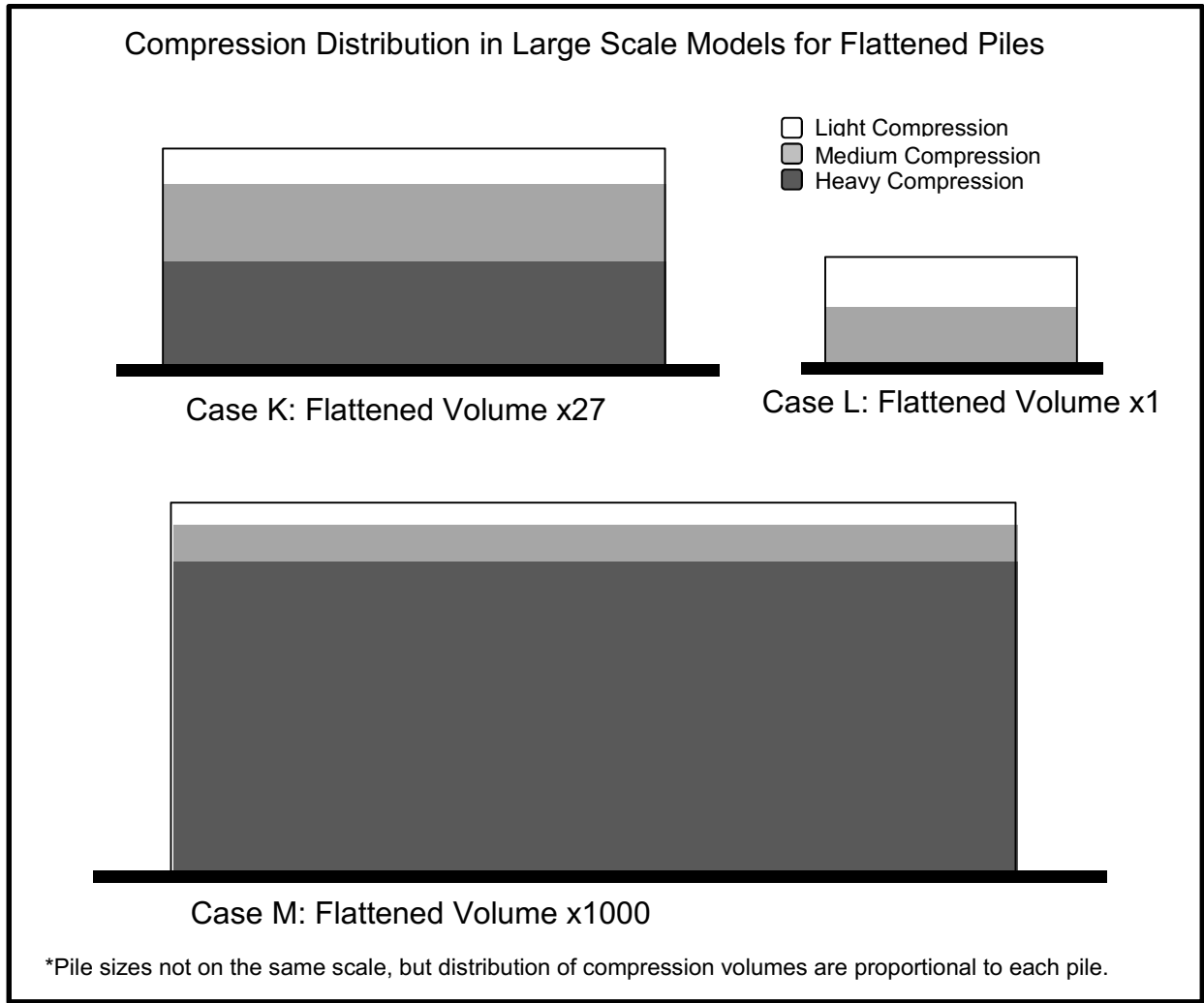


Figure 20: Graphic models of compression distribution in the predicted flattened piles of Table 6.

Monte Carlo Simulation of Mass Estimates Improved by Averaging Method

Using the statistical data gathered in phase II, multiple mass estimates were generated using a normal distribution generator. This simulates measuring the chip pile 10,000 times for each case examined. Table 7 and 8 show statistical summaries of these simulated estimates for both conical and flattened

shape piles. There are three cases generated for each pile shape. First, 10,000 single mass estimates were generated that matched the average and standard deviation of the original ten estimates generated in phase II. Then an additional 10,000 iterations of mass estimates were generated using the average of five random single mass estimates and the last 10,000 values were generated using the average of ten random single mass estimates. This resulted in three sets of estimates, with each set having 10,000 mass estimates. When the 10,000 estimates for each case were averaged out, the accuracy of the mass estimates did not improve, but the precision error was significantly improved as indicated by the standard deviations. Closer examination of the conical shaped pile data, shows that averaging multiple single estimates, improved the chances of the final value to be within $\pm 5\%$ of the actual mass to be over 92.7% with just averaging 5 estimates together, and improving the number of estimates to be within $\pm 3\%$ from 40.5% to over 70.4%.

Table 7: Chart showing the total average, standard deviation, and percentage of the 10,000 Monte Carlo simulated estimates which fall within 3% and 5% of the actual mass when the predicted masses have been generated using the average of multiple estimates of conical piles.

Descriptive Statistics	Iterations Using a Single Mass Estimation	Iterations Using an Average of 5 Mass Estimations	Iterations Using an Average of 10 Mass Estimations
Average Error Percentage	-1.59%	-1.58%	-1.57%
Standard Deviations	5.4%	2.3%	1.7%
Percentage within an accuracy of $\pm 3\%$	40.5%	70.4%	80.2%
Percentage within an accuracy of $\pm 5\%$	62.5%	92.7%	98.0%

The same procedure was applied to the flattened pile data with similar results. Averaging multiple mass estimates improved the chances that the final

value will fall within $\pm 5\%$ of the actual mass over 81.1% of the time with just an average of 5 separate estimates. The only difference is with answers that are $\pm 3\%$ of the actual mass. The number of answers that fall within that range does not improve with just 5 averages, and when averaging 10 estimates it actually worsens by 0.6% when compared to single mass estimates.

Table 8: Chart showing the total average, standard deviation, and percentage of the 10,000 Monte Carlo simulated estimates which fall within 3% and 5% of the actual mass when the predicted masses have been generated using the average of multiple estimates of flattened piles.

Descriptive Statistics	Iterations Using a Single Mass Estimation	Iterations Using an Average of 5 Mass Estimations	Iterations Using an Average of 10 Mass Estimations
Average Error Percentage	-3.27%	-3.36%	-3.35%
Standard Deviations	4.1%	1.9%	1.3%
Percentage within an accuracy of $\pm 3\%$	41.0%	42.4%	39.4%
Percentage within an accuracy of $\pm 5\%$	64.2%	81.1%	89.8%

Calculating Error of Operator

To determine what percentage of the error is due to operator error an image set of a chip pile is processed 3 times using the same ground control points (GCP), the same procedures, and the same software. This was repeated using four different image sets. The height and volume of the chip pile was compared to the mean value of the set to see the deviation generated by the operator's procedure. The results shown in Table 9 of an operator manually entering GCP, or coordinates, can on average introduce a standard deviation of about 1.8% in the height or Z axis, and skew the volume by a standard deviation of about 2.4%.

Table 9: Comparison of the variation of answers when the same photo set is reprocessed using the same procedure to examine deviation due to operator error, both in the Z axis and in the X,Y,Z axis.

Descriptive Statistics	Height of the Pile (Z Axis)	Volume of the Pile (X,Y,Z Axis)
Standard Deviation	1.8%	2.4%
Maximum	2.9%	3.8%
Minimum	-4.1%	-5.5%

Calculating Error due to Software

Using the fifteen image sets, two estimates were generated for each set. One estimate was generated using PhotoModeler Scanner software with GCP for scale, and a second estimate was generated using Agi-Soft with the scale of the model determined based on altitude of the drone and camera specifications. Each pair of estimates was compared to the other and the difference between estimates were analysed. The statistical differences are summarized in Table 10. Over the fifteen image sets, an average of 2.34% difference was detected between the estimates of the two software packages. The differences covered a range of 15.74%, which had a standard deviation of about 3.96%.

Table 10: Chart showing descriptive stats of the difference between estimates generated using different software processing identical image sets.

Average Difference	2.34%
Standard Deviation	3.96%
Over Estimated Difference (Maximum)	9.53%
Under Estimated Difference (Minimum)	-6.21%

Compensation Error due to Decompression

Based on the percentages and range of decompression shown in Figure 10, an illustration of two cross-section models is presented in Figure 21. It demonstrates how compression differs between chip piles, which have undergone decompression, compared to a normal chip pile without decompression. Notice the difference between the piles is at the surface wood chips directly under the cells removed from the top of the pile. These cells experience a partial decompression after the removal of the four cells of wood chips. These models predicted pile N experiencing a volume loss of 4.9% while pile O has a volume loss of 5.8% after the removal of the top of the conical pile.

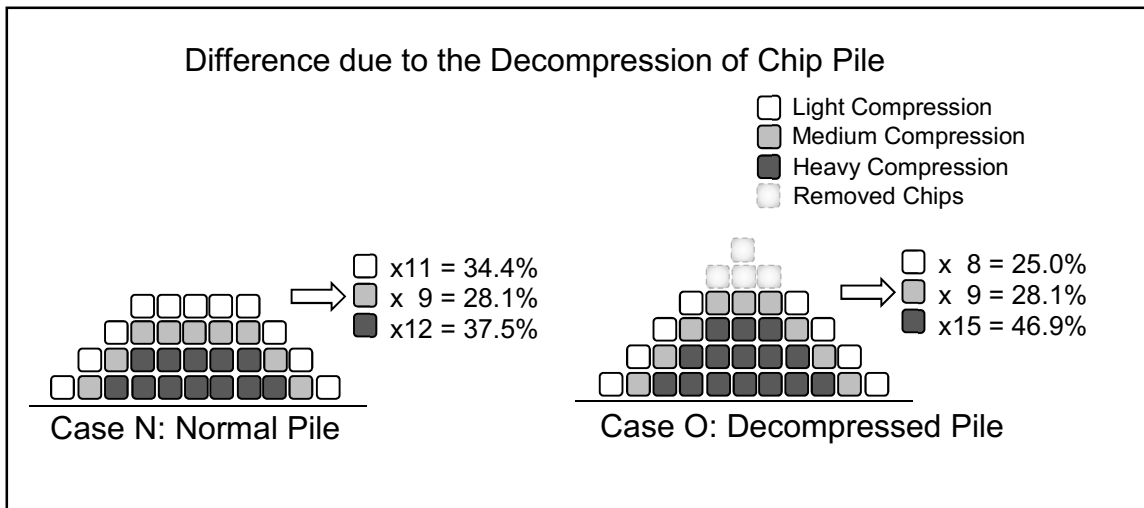


Figure 21: Showing the different varying densities of wood chips as one pile goes through decompression while the other pile is formed normally.

DISCUSSION

DEVELOPING THE CONTROL METRICS AND VARIABLES

During the exploratory experiments of phase I, there were various metrics collected to use as benchmarks for the estimates, or as controls to determine if they affected the final mass estimates. Some of these variables did not affect the mass estimations, while others could be bundled or summed up into a single variable. Each variable was analysed and the reason to use or omit them from the final equation is explained below.

Chip size composition of the pile is monitored by the mill acquiring the wood chips. As long as majority of the pile conforms to the mill's standard, it will not skew the results. The chip size affects the compression characteristics of the pile and since the compression curve has been calibrated to each mill's chip size composition, any slight deviation in sizes that is acceptable to the mill's standard will not generate significant errors. That said, I suggest to develop a new compression curve for each mill for calibration purposes, or if the material is of a different nature, such as hog fuel or wood pellets for example.

Moisture content changes the mass of the chips (Mullins and McKnight 1981) in the pile, and mass of the chips affects the depth at which maximum compression occurs in a pile, but because bulk density accounts for moisture

content (Mullins and McKnight 1981) and the density of the wood base on species (Mullins and McKnight 1981), it is unnecessary to incorporate all these factors as separate variables in the conversion formula. Moisture content was only required when estimating oven dry wood fibre mass, as using bulk density values will predict the pile's green mass. The bulk density value takes into consideration the moisture content of the wood chips, density of the wood based on species, and any variation in the ratio of wood chips versus void space in the measured pile. Hence, bulk density can be used to replace all three other variables in the conversion formula.

When measuring bulk density, it is possible to acquire a loose bulk density value, which is defined in this study as the bulk density of wood chips under minimal compressive forces; or an ASTM standard bulk density, which is the density of the wood chips that has been tapped and settled into a container as per the ASTM standard. A standard bulk density measurement requires some compaction of the material being measured as part of the procedure requires dropping the box from a height defined in ASTM C29/C29M Standard Bulk Density (ASTM International 2016). While the hypothesis was based on estimates using an uncompressed wood chip density, this is not achievable in practice. Volume measurements of the wood chips in the one-meter tall HDPE container or a 44-imperial gallon drum have some settling and compaction inherent to the measuring process. This means the compression curves are actually developed with some settling and compression incorporated into these

values and curves, hence the use of ASTM bulk density is preferred due to the benefits of following a standard. In the attempt of measuring loose bulk density of the wood chips, it was noted that these values acquired were not reliable. They can vary by as much as 10% between measurements, even if using the same chips measured several times in the same container. In phase II, the bulk density used was a semi-loose bulk density measured from the total volume and mass of the whole chip pile, but future phases only used ASTM C29/C29M Standard Bulk Density method (ASTM International 2016). The benefit of using this standard is twofold. First, the bulk density values obtained using this method is consistent, compared to measuring a loose bulk density, thereby removing the 10% precision error. Secondly, this international standard is already in use by the industry and does not require retraining technicians to acquire an accurate 'loose bulk density' value. The improvement in precision of the bulk density values when using a standard bulk density measuring method makes any difference between compressed and uncompressed bulk density a minor variation that can be accounted for in a calibration process. This is a case where precision is more important than accuracy, as accuracy can be corrected in a later stage, but precision errors results in an uncertainty error of the final estimate.

VOLUME LOSS DUE TO SHAPE, HEIGHT AND BULK DENSITY

The hypothesis of this thesis assumed that bulk density would vary throughout a chip pile depending on the amount of compressive pressures applied from above by the layers of wood chips. The models in Figures 16, 17, and 18, show how varying height, shape, and bulk density will vary the compression forces distributed within the chip pile. These variables are actually interrelated with each other, as all three variables are different applications of the same gravitational force on the chip pile. For example, changing the height of the pile will also change the shape of the pile, but to understand how these different characteristics effect the compression individually, these variables are examined as separate models. This makes it easier to understand the effects of compression due to each of these variables.

In each pile, each cell can be under the influence of light, medium, and heavy compressive forces. The white cells are under light compression forces, which have little to no loss of volume. These cells can be converted to generate an accurate estimate of the fibre mass based on the standard bulk density value alone without any other compensation factor. The light grey cells represent medium compression, which on average has a loss of 5% in volume. Estimates of these volumes will generate a shortage in mass estimates of about 5% due to the increase in bulk density in this zone. The dark grey cells are subject to heavy compressive forces from the light and medium cells above them. Each of

these heavy compression cells are under max compression, and an estimation of fibre mass for these cells will be 9.46% short of the actual mass per the maximum volume loss found in Figure 11. Notice that most of the models presented in Figures 16, and 17 have piles with a size of 16 cells stacked in different configurations. While their overall sizes are the same, they have different quantities of light, medium, and heavy cell compressions. These variations in compression distribution skew the final mass estimates by a percentage of 2.5% to 7.7%. This is calculated by summing up the percentage of volume compensations for all the cells in the pile and dividing that by the total number of cells in the pile. The overall percentage of volume change for a pile configuration is the value that is applied to the compression compensated conversion Equation 4 as variable C.

All the cases found in Figures 16 and 17 attain maximum compression after a depth of two cells, whereas Figure 18 examines compression differences of wood chips with different standard bulk densities. Notice that in case G due to the lighter wood chips it takes twice the number of cells to reach maximum compression. These models simulate two bulk density wood chips, where one pile has a standard bulk density that is twice as heavy as the other pile. This may be due to species of the wood, moisture content of the chips, different chip size composition that changes the void ratio in the chip pile, or a combination of the three factors. The variation of compression forces in the piles, results in different volume loss even though both piles occupy the same overall volume.

DECOMPRESSION REQUIRES AN ADDITIONAL CORRECTION FACTOR

Another factor that complicates conversion from volume to mass is when incorporating chip piles that have undergone a compression followed by a decompression stage. One of the experiments examined the decompression of wood chips, which was mapped on a graph in Figure 10. The data is spread out over a range of values and not a linear relation between volumes recovered versus time. While the data shows an immediate volume recovery of 31% to 44% after a compression load was removed, this was only a partial volume recovery. The final volume recovered after an hour was in the range of 36% to 56%, at which point the wood chips have reached a new equilibrium and no further improvement was noticed without manual intervention. When the wood chips were manually loosened up it returned to the original volume prior to the application of the compression load. This indicates that the chips were not damaged during the compression process. It was assumed that during unassisted decompression the wood chips are interlocked or entangled with its neighbouring chips and do not allow the pile to recover to the original void spacing prior to compression. It requires manual decompression to recover the original void spacing.

This creates a problem for converting volume to a mass estimate. Since the original CCC formula is calibrated to the original void spacing for a chip pile with only one compensating variable to account for natural compression within

the chip pile, it does not take into consideration the additional volume loss due to the pile not fully decompressing. Even if a second correction factor was incorporated into the CCC formula to compensate for decompression, at the moment there is no accurate method of determining this exact value other than to take an median value from the range of volume recovery. With a range of 36% to 56%, the middle value that is used for all decompression cases would be 46%, but this would be a rough estimate. This 46% recovery is a percentage of the maximum compression volume loss (9.46%). Hence, the 46% decompression recovery translates to 4.35% volume recovery of the maximum 9.46% volume loss due to compression. This means any cell that was affected by decompression will experience an additional 5.11% volume loss per cell in addition to any normal volume loss determined by the CCC method.

As an example Case N and O in Figure 21 models a difference in chip density depending on whether there was previously loaded chips over the pile. In this example both piles have the same volume. While case N will have a predicted volume loss of 4.9%, due to the removal of 4 cells from the conical pile, case O has a predicted volume loss of 5.8%. In this example the overall increase in volume loss due to decompression is only 0.9%, but other configurations may yield different volume differences for a pile that has undergone decompression factors.

STABILIZATION PERIOD REQUIRED FOR ACCURATE MASS ESTIMATION

The experiments performed in phase I, determined that a settling or stabilizing period is a necessary step prior to the image collection stage. Allowing the pile to settle before collecting volume imagery will reduce accuracy errors. The results from the experiments shows that a pile requires 180 minutes after introducing new loads, and 30 minutes after removal of compression loads before the pile has sufficient time to settle and stabilize. Since the formulas generated to convert volume to mass are calibrated for a stabilized state, it is important to allow this settling stage to occur, or the final estimates will be inaccurate. By skipping this stage newly created piles will be larger than a settled pile generating an over estimation of the mass, and piles without proper decompression periods will generate an under estimation of the mass.

Based on Figure 9, it is evident that measuring the volume immediately after loading the pile with new material would skew the mass estimates by as much as 39% of the volume of the newly added material. Table 9 shows in some cases, piles can achieve fully stabilized compressed state immediately after a new load was added, but majority of the cases requires up to 3 hours before reaching a fully stable state. Whether it is BLC, CCC, or a proprietary method used by the mills to convert volume to a mass estimate, these formulas have been calibrated for a stable state pile. Measuring the volume prior to this stable state will introduce skew into the estimate by as much as 39% of the

volume of the new material loaded onto the pile. To accommodate volume measurement and mill operations, I suggest measuring volumes of chip piles in the morning before the first truckload has been unloaded onto the pile. The volume of the existing chips in the pile should be at its most accurate for the calibrated formula after having the night to settle into a stable state.

DIFFERENCES BETWEEN BASIC LINEAR CONVERSION METHOD (BLC) AND COMPRESSION COMPENSATED CONVERSION METHOD (CCC)

As shown in Equations 3 and 4, the only difference between the BLC, and CCC method is a single compensation factor $(1 + C)$ where the C variable represents the total percentage of volume loss in the pile due to compression. For example, if we look at case C in Figure 16 where the chips are held inside a silo, we see that it has an estimated volume loss of about 7.7%, which makes the compensation factor C equal to $(1 + 0.077)$. This suggests that the mass of the chips is actually 1.077 times the predicted mass based on bulk density of the chips and internal volume of the silo. The reason for this increase is because the compensation formula takes into account that the measured bulk density is not under high compressive forces, and since most of the chips in the silo are under high compression, this factor accounts for the volume loss due to compression differences. This is a suspected reason that the mills are underestimating the mass of their inventory in their yards. As the piles get larger and taller, more chips are compressed into the spaces used for storage. This

underestimation could show up as a shortage of chips delivered from field operations or as an inefficient processing of the chips by the mill. This loss of volume can also be seen in uncontained piles, since the external layer of chips can act as a force holding the interior chips together under pressure, similar to a container or a silo wall. Hence, in cases D to G in Figures 17 and 18, the volume loss can also be calculated even though the piles are not contained within a structure.

APPLICATION OF METHOD IN A MILL ENVIRONMENT

The CCC method developed during phase I and II were applied to chip piles at a local mill. By comparing the estimated mass with the values supplied by the mill, it is possible to determine if the method used by industry is similar to the CCC method. The results in Table 5, shows that between the two methods there is a calculated difference of about 1.4%. This suggests that on a medium chip pile scale, the formulas used by the mill behave similarly to the CCC method. If the data is further separated into pile types, estimates of pile C, which is a flattened shape, are more accurate than estimates of piles A or B which are conical shaped. There is on average only a 2% difference between methods for the conical shaped piles, which is definitely a small error compared to the volume error incurred during the volume surveying stage. Being that these medium size piles are many factors smaller than most piles on a mill site, an

exploratory analysis was also completed to examine accuracy on large-scale chip piles.

To extrapolate for large piles, a couple of the medium size piles were scaled up for analysis. In all the cases, it was assumed that all other factors such as species, chip size, moisture, etc. remain identical. Only the quantities of wood chips were increased. The results shown in Table 6, predicts on average an increase in error of about 5% when the volume was changed. Even flattened piles that were previously showing a high degree of accuracy with only 0.3% difference now revealed a difference between methods of estimation by at least 3.5% (Flatten Volume x27 percentage in Table 6). It is assumed the mills have calibrated their formulas to be accurate at the medium size test piles but do not take into consideration the variation of density when increasing the volume of their chip piles. Therefore, the results simulated on mass estimates on large-scale piles can be off by about 5%.

The difference of compression due to scale can be seen when modeling the piles graphically. This is shown in Figures 19 and 20 as the percentage of the pile that is under heavy compression changes drastically when scaling from the mill's medium size piles (Case I and L) to larger size piles. In these medium size piles there are minimal areas of the pile that is under heavy compression, with over 75% of these piles composed of medium and light compression. In the flattened pile Case L, there is only medium and light compression, which

explains the 0.3% oven dry mass prediction difference between the CCC method, and the mill's conversion formula. In the conical pile Case I, there is a small amount of heavy compression area in the pile. This is the reason that the conical pile generates the 2% difference between the two methods of mass estimation.

When the models of the larger piles (scaled by 27 and 1000 times the size of the mill's calibration chip piles) are modeled, notice that majority of these piles consist of heavy compression areas. This confirms the increase of the 3.5% to 5.5% difference between mass estimation methods, as the mill's linear formula does not account for the increase of heavy compression areas. Since their main chip piles are closer to this scale of chip piles, the mass estimates using the formula calibrated to the medium size piles will fall to account for this change. The good news is that once the compression variation for a specific pile shape, size, and wood chip properties are determined, a correction factor can be applied to the existing mill formula to mitigate this scale error.

ERROR DISTRIBUTION IN VOLUME MEASUREMENTS AND MASS ESTIMATIONS

To improve accuracy of wood chip mass estimations, every stage from surveying the pile, to the conversion of the volume to a mass estimate was examined. It became obvious that while volume to mass conversion was the

focus of the thesis it was not the major source of error. Based on the compression curve (Figure 11) the maximum loss of a pile volume is 9.46%, with most of the practical results from the small-scale piles to the larger mill piles falling in the range of 1% to 6%. Therefore, by applying the CCC method to any chip pile will at most improve accuracy by about 6%. Whereas volume measurements of the pile have generated about 10% error in the 3D capture process (Table 1), up to 5.5% error from operator input (Table 9), up to 9% error from software bias (Table 10), as well as a host of other errors such as GPS coordinates of GCP. Compounded, these errors can potentially generate over 20% error in mass estimates, if the errors are at the extreme range, and all the errors are skewed in the same direction. This error can be so large that an experienced technician or supervisor may even detect the error based solely on a visual inspection of the pile. However, on average, the errors generated are usually smaller than the above listed maximums, as errors from different aspects may be biased in different directions, thereby partially cancelling each other out. But the fact that it is possible to have large errors compounded together to cause even larger skews of accuracy, means that effort to control and manage volume measurement errors will have a greater effect on estimated mass accuracy than the incorporation of CCC method of volume to mass conversion. While this thesis was originally focused on improving volume to mass conversions, it will suggest methods of improving accuracy of volume measurements based on errors noticed during the experimental process of measuring the chip piles.

Volumetric error as noted during phase II of this research is a concern that needs to be managed. The volume of a single chip pile when surveyed multiple times resulted in varying volumes which were skewed to a range of 18% between maximum and minimum values, as shown in Table 1. This error is generated from a combination of using different image sets with known GCP for each volume measurement. Volumetric error is also visible within an exploratory experiment to compare volume error between two software packages. The differences generated a range of 16% as shown in Table 10. This time the contribution to the error is due to different algorithms in the software packages, and the method of determining the scale of the 3D model. The PhotoModeler values were generated using distances of known GCP; whereas the AgiSoft values were generated using known camera specifications and drone flight heights to calculate the scale. Regardless of how these volume errors were generated, the solution to reducing these precision errors is to take multiple volume measurements and averaging them to get a final value. As shown in the Monte Carlo Simulations on Tables 7 and 8, while averaging does not change the accuracy error of the estimates it does improve the precision error as indicated by the standard deviation (SD) values. A single image set can produce a value with a 4% to 5% SD, whereas averaging as little as five sets of images improves the SD down to about 2%. The SD is further improved down to about 1.5% when averaging ten or more image sets together. This reduction covers variation in the image sets, errors in the coordinates of GCP, errors in GPS

data, differences in software algorithms, and any other precision error that may occur when generating volume measurements.

This is further confirmed when looking at the number of 10,000 simulated mass estimates that fall within $\pm 5\%$ or $\pm 3\%$ of the actual mass. In all cases except for one, averaging greatly improves the number of estimates that are within the two chosen percentile ranges. The only one that failed to improve the precision after averaging multiple masses was the case with the flattened pile and requiring the estimate to be within $\pm 3\%$ of the actual mass. The precision only slightly improves after averaging five estimates, and actually drops by the time ten estimates were averaged together. This failure to improve precision has to do with the accuracy of that data set. Since the mean of the dataset has an error that was greater than -3% . By improving the precision of this set of estimates it actually decreased the accuracy by skewing the estimates towards the -3% value. Fortunately, by adding a calibration constant to the equation to correct for this accuracy error, it will correct the skew generated by the averaging method on this data set.

While the averaging method needs multiple image sets, this does not require multiple flights of the UAV drone, as suggested in the methodology. By capturing a dense grid of images with greater than 80% overlap between the images, will allow a randomizing selection method to generate different image sets from a single flight. There are two criteria to keep in mind when generating

multiple image subsets. The first is to ensure enough images are included in each subset to have full coverage of the chip pile. The second is to generate enough image subsets that will balance between generating a final volume that has a high precision confidence while taking into consideration the hardware capabilities of the computer system to be able to generate the models in a timely fashion. On average, using a single high-end computer will take about five to ten hours to generate a 3D model of a medium sized chip pile. The time range is highly dependent on the number of photos in each set. Some surveying companies in the industry have used a network of computers to distribute the computing task, reducing the processing time down to a couple of hours even for larger image sets.

To optimize the processing time and minimize the precision error requires minimizing the number of photographs and maximizing the number of photo subsets. Most software packages prefer that each point calculated to appear in at least three images for reasonable accuracy when determining the X,Y,Z coordinates of each point of the point cloud. Since the images have at least 80% overlap, it means any point on the chip pile should show up at least five times per pass. This means if two images are removed from every string of five consecutive images, the remaining images should still cover each point at least three times. It is possible to reduce a flight with 100 images down to 60 images and still maintain the ratio of three photographs per series of five consecutive images. This allows images from a single flight to have the number of images be

reduced by 40% for each subset. By varying which 40% is removed for each subset will allow the generation of the ten or twenty image subsets desired for volume averaging. This is by no means the only way to optimize the image sets, as any variations that still adhere to the rule of maintaining three images per point of interest could work. The method used should be determined by the operator with the capabilities of the computer processing system in mind. In the end, as long as the method applied is without bias to all subset images, the error in the final estimate will be minimal after it has been averaged together.

Accuracy Errors due to Image Scale Calibration of the 3D Model

To improve the accuracy of volumetric measurements, proper scale needs to be entered into the model. Scale can be introduced through several different methods. The preferred method is to perform a precision ground survey of GCP using traditional survey equipment such as total stations. Location of GCP can be mapped using high accuracy GPS units. Alternatively, another method to determine scale is to apply camera specifications and UAV flight elevation to calculate the X and Y scale of the image. While all the suggested methods will generate a scale for the model, the method capable of millimeter range accuracy is the ground survey method. In addition to having high accuracy, ground survey methods will also consistently have a low precision error. The other two methods, which are dependent on satellite signals, can run into issues depending on positions of the GPS satellites when the coordinates

are taken. Interference from surrounding features on the GPS signal, as explained in the literature review will effect GPS accuracy. While GPS is a more convenient method to collect data and has the possibility of being able to be incorporated into the data automatically within some software applications, the larger precision error, and an accuracy of several centimeters does not make this a preferred method. Figure 22 shows GPS coordinates collected during an aerial flight after it has been corrected by GCP. The arrows show the corrections exaggerated by a thousand times. Since it required GCP to correct the GPS coordinates it stands to reason to use GCP in the first place for scale accuracy, and skip the correction stage needed by GPS coordinates.



Figure 22: Sample of GPS error when compared to ground control points exaggerated by 1000 times

Accuracy Errors due to Software Algorithms for Generating 3D Models

Finally, a look at the differences or errors generated based on software algorithms required another exploratory experiment. In Table 10, two software packages measured the volume of the 3D models and the statistical differences between the results generated by the two were analysed. The PhotoModeler software determined scale using manually entered GCP, while AgiSoft applied a scale to the model using the camera specifications and the drone's altitude as reported by the on board GPS unit. Since both cases used the same photo sets, the differences in the volumes were solely due to scale of the 3D models and software algorithms. These volume differences identify that the scale precision needs to be scrutinized and tightened down, as having a range of 15% variation between software measurements is unacceptable. The choice to use PhotoModeler Scanner was due to a single publication regarding its capability to generate a high positional accuracy, although this is not necessarily the best solution. More studies are needed to examine why one algorithm is so vastly different from another that it generates up to a 15% variation when the same image set is fed to both software algorithms. Moreover, this error needs to be further studied, as this error will skew the final inventory estimates by millions of dollars.

CONCLUSION

This thesis has explored many aspects of remotely sensed estimates of wood chip inventories, and while it has exposed many errors that can skew these mass estimates, it is not meant to suggest that any fibre mass estimation from remote surveying is unreliable or expected to be inaccurate. In these experiments, multiple precision and accuracy errors have been identified and addressed. If the multiple factors that introduce precision errors are assumed to follow a normal distribution, it is very likely that these errors will mostly cancel each other out reducing the overall error most of the time. Therefore, on a regular basis, estimates of chip inventory can be accurate, but to eliminate the possibility of occasional compounded errors skewing the resultant estimate by a large amount, the following procedures should be implemented.

1. Images of the chip pile should only be taken after the pile has had a chance to settle and stabilize.
2. A period of at least 3 hours settling time should be observed before capturing the images.
3. To minimize interruptions of mill operations the images should be taken first thing in the morning, after a night of settling has occurred, and before

mill operations begin for the day such as new wood chip deliveries, or wood chips removed from the pile for use in the mill.

4. The chip pile should have multiple samples measured for ASTM bulk density values, and moisture content.
5. These density and moisture content values should be averaged to improve precision and lower conversion errors.
6. The chip pile should be captured using an overhead UAV, and the grid of images captured should have a high degree of overlap between photographs to allow for transforming a single flight into multiple image sets of randomly selected photographs.
7. It is expected that at least ten image sets will be required for averaging to improve the confidence of the final mass estimate. Each of these image sets should still have full coverage of the whole chip pile from various angles.
8. Multiple GCP should be identified in each of the image sets to provide the software with proper scale for each 3D model generated and these control points should be surveyed using a highly accurate, ground-survey method to minimize accuracy error.

9. Volumes generated by each image set should be processed by the CCC method to improve accuracy of the mass estimates.

10. Estimates from multiple image sets should be averaged together to improve the overall precision of the final estimate and reduce error generated from the multiple stages of this process.

By taking these precautions, it should be possible to improve accuracy of the mass estimates, but more importantly the precision and confidence of the results. Overall, it is possible to use remotely captured images to generate a volume and using the CCC method to convert this volume to a mass estimate. In its present form, it will improve the estimates compared to methods used at the mills in the industry, but there is stillroom for further refinement to improve accuracy and new techniques are required to improve calibration of the system.

LITERATURE CITED

- Arnold, Lisa L., and Paul A. Zandbergen. "Positional accuracy of the Wide Area Augmentation System in consumer-grade GPS units." *Computers & Geosciences* 37 (2011): 883-892.
- ASTM International. "Standard Test Method for Bulk Density ("Unit Weight") and Voids in Aggregate." 2016.
- Brockbank, R., and J. M. Huntley. "Contact Force Distribution Beneath a Three-Dimensional Granular Pile." *Journal De Physique II*, no. 10 (1997): 1521-1532.
- EOS Systems Inc. "Quantifying the Accuracy of Dense Surface Modeling within PhotoModeler Scanner." *PhotoModeler*. Sep 20, 2012. info.photomodeler.com/blog/photomodelers-dense-surface-modeling-accuracy-study (accessed Oct 2014).
- Gale, Robert. "Environmental costs at a Canadian paper mill: a case study of Environmental Management Accounting (EMA)." *Journal of Cleaner Production* 14 (2006): 1237-1251.
- Hudson, James M.S. *Processing Large Point Cloud Data in Computer Graphics*. Doctoral Dissertation, Doctoral dissertation, The Ohio State University, 2003.
- Liffman, Kurt, Myhuong Nguyen, Guy Metcalfe, and Paul Cleary. "Forces in piles of granular material: an analytic and 3D DEM study." *Granular Matter* 3 (2001): 165-176.
- Lindgren, Ralph M., and Wallace E. Eslyn. "Biological Deterioration of Pulpwood and Pulp Chips During Storage." *TAPPI* 44, no. 6 (1961): 419-429.
- Mullins, E. J., and T. S. McKnight. *Canadian woods : their properties and uses*. Toronto: University of Toronto Press, 1981.
- Oron, G., and H. J. Herrmann. "Exact calculation of force networks in granular piles." *The American Physical Society* 58, no. 2 (August 1998): 2079-2089.

- Strecha, C. , W. von Hansen, L. Van Gool, P. Fua, and U. Thoennessen. "On Benchmarking Camera Calibration and Multi-View Stereo for High Resolution Imagery." *Computer Vision and Pattern Recognition, IEEE Conference*. Anchorage, AK: IEEE, 2008. 1-8.
- Trofymow, J. A., N. C. Coops, and D. Hayhurst. "Comparison of remote sensing and ground-based methods for determining residue burn pile wood volumes and biomass." *Canadian Journal of Forest Research* 44, no. 3 (March 2014): 182-194.
- Walford, Alan. "A New Way to 3D Scan." *Visualisation Technical* (Position IT), Nov / Dec 2009: 56-60.
- Wing, Michael G., Aaron Eklund, and Loren D. Kellogg. "Consumer-Grade Global Positioning System (GPS) Accuracy and Reliability." *Journal of Forestry*, June 2005: 169-173.
- Witte, T. H., and A. M. Wilson. "Accuracy of non-differential GPS for the determination of speed over ground." *Journal of Biomechanics* 37 (2004): 1891-1898.
- Witte, T. H., and A. M. Wilson. "Accuracy of WAAS-enabled GPS for the determination of position and speed over ground." *Journal of Biomechanics* 38 (2005): 1717-1722.